The positioning of the distributor plate relative to the plenum space is illustrated in Figure 5.4. The bottom of the distributor plate is at the appex of the plenum. This creates a very small dead volume between the plenum and the distributor plate.

The catalyst section and gas-exit section are identical in internal dimensions to the reaction zone and product gas-exit zone of the microreactor used for steady-state F-T synthesis studies (Section 4.1.1.2). The catalyst zone consists of a 3.175-mm wide slot, milled 25.4 mm long in the 14.29-mm deep catalyst section. The ends of the slot are milled round, so that no corners exist to trap the catalyst. The gas-exist zone consists of a slot (3.175 mn × 6.35 mm × 25.4 mm) milled from the bottom surface to match the slot cut in the catalyst section. A recess identical to the one milled in the base section holds the sintered stainless-steel catalyst retention plate. A 1/4-inch O.D. tube extends down into the gas-exit section from above breaking through to the slot.

The external dimensions of this microreactor are approximately 101.6-mm long, 50.8-mm tall and 25.4-mm wide.

The three sections (zones, i.e., the plenum zone, the reaction zone and the gas-exit zone) are held together by four 10-32 Allen head-cap screws. A gas-tight seal is maintined between the sections by using silicone rubber during assembly. A 1.59-mm clearance hole extends into each section, allowing the sampling capillary to be inserted into any one of the three zones. When not in use, these holes are filled with 1.59-mm rods which are swaged in place for a leak-proof seal.

5.1.1.3 Solenoids

Two solenoids control the sliding movement of the brass plug in the plenum zone. Each solenoid consists of a 216-mm long piece of 1.2-inch O.D. 316- stainless-steel (non-magnetizable) tubing with a 0.049-inch wall thickness. The winding begins 44.5 mm up from the base of the tube and is 108 mm in total length. The winding contains 2,830 turns of number 23 AWG copper solenoid-winding wire, producing a minimum force of 1.33 N at the start of the plunger stroke.

An adjustable carbon-steel (magnetizable) stop extends down into the tube and the winding area. The stop causes the flux lines of the magnetic field to be re-directed so that the force on the plunger increases greatly as it approaches the stop.

The plunger itself is a 10.0-mm diameter piece of carbon-steel, 76.2 mm in length. Two 3.175-mm wide grooves, 1.27-mm deep, have been milled the length of the plungers in order to keep gas from being compressed in front of the plungers when the solenoids are activated. A small nipple, 3.23 mm in length, has been machined into the lower end of the plungers. A small hole has been drilled in these nipples in order to attach a 0.356-mm wire that controls the sliding-plug movement.

The solenoid windings are electrically connected to a relay which controls the power input to each solenoid. In particular, one solenoid is on while the other is off. Inside the soleniod that is on (solenoid "L" in Figure 5.1), the plunger has been drawn upward nearly co.:·] in contact with the plunger stop. The force on the plunger at

this point is very high. This creates tension on the wire connecting

the plunger in the actuated solenoid to the sliding plug. The sliding

plug, in turn, is drawn up tightly against the seat created by the

O-ring. The other, de-energized solenoid (solenoid "R" in Figure 5.1)

is, at the same time, resting at the base of the solenoid tube.

The wire connecting this plunger to the other side of the sliding

plug has several millimeters of slack in it so as not to keep the plug

from seating. When the relay is switched, solenoid R is energized and

solenoid L is de-energized. The plug is drawn from left to right and

seats against the right-hand O-ring. Both solenoids are kept cool

using small fans in order to maintain a maximum force on the plungers.

5.1.1.4 Valve and Solenoid Switching Circuit

The solenoid valves and solenoids control whether argon or helium

is being fed to the catalyst zone of the sliding-plug vibrofluidized-

bed microreactor. Solenoids L and R shown in Figures 5.1 are

alternately actuated through the use of a 24 volt relay. The power

inputs to the solenoid valves, solenoids, and this relay are all

provided by a 24-volt power supply.

Switching of the solenoid valves 1 and 2 as well as the relay is

accomplished through the use of a Heath H-89 microcomputer and a

parallel-port computer interface. Figure 5.6 is a diagram of one

circuit of the interface. One such circuit is provided for each valve

or relay. A transistor-transistor-logic (TTL) signal (0 or 5 volts)

is produced at the parallel output port by the microcomputer. The

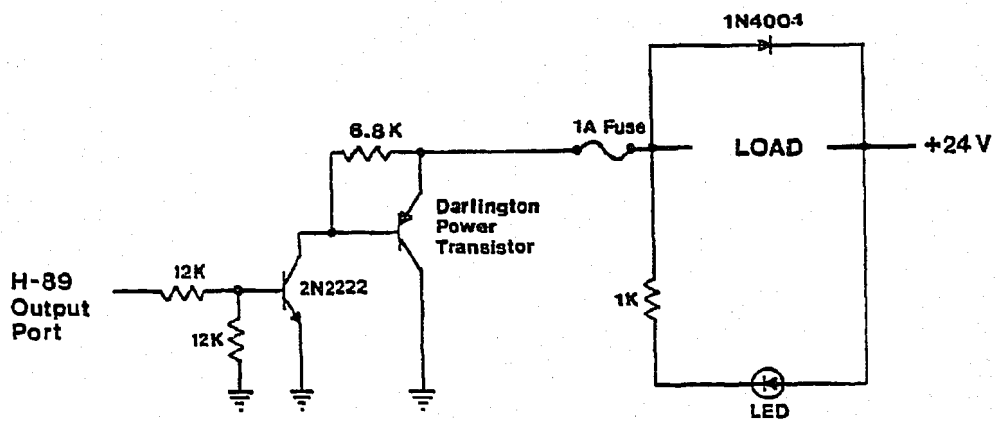interface then uses this signal to determine whether 0 volt or +24

Figure 5.6. A Diagram of One Circuit in the Interface
Between the Experiment and the H-89 Micro-
computer Parallel Port.

volts should be supplied to the solenoid valve or relay. The 2N2222 transistor amplifies the signal from the computer so that it can activate the Darlington power transistor. When activated, the power-transistor output drops from 24 volts to 0 volt. This, in turn, causes a 24-volt drop across the coil of the solenoid valve or relay (LOAD), inducing the valve to open or the relay to switch.

5.1.2 Materials

The material used as the fluidization media in the cold-flow model studies was -150-300 μ fused-iron catalyst. This catalyst was described previously in Section 4.1.2.1. The gases used were prepurified grade argon, helium and nitrogen supplied by Airco.

5.1.3 Experimental Procedures

5.1.3.1 Cold-Flow Microreactor Model Loading

The base section of the sliding-plug vibrofluidized-bed microreactor was first attached to the suspension apparatus. A distributor plate made of sintered stainless-steel was then fitted into the recess in the base section. Several distribution plates of different porosities were used over the course of these experiments. Silicone rubber was used as a gasket material between the sections of the cold-flow model. A bead of silicone was placed around the edge of the distributor plate in contact with the lexan. The silicone was allowed to set for several minutes and the catalyst section of the model was then put in place making certain that no silicone flowed into the catalyst zone. At this point, the silicone was allowed to dry for

at least two hours. One gram of the fused-iron catalyst was weighed out and poured into the reaction zone.

The gas-exit zone, containing a 20μ catalyst retention plate was affixed to the catalyst section in a similar fashion. The silicone rubber gasket material was allowed to cure for twenty-four hours. The four bolts that held the three sections of the cold-flow model together were then inserted and tightened. Care must be taken not to overtighten these bolts. Only a thin piece of lexan lies between the distributor plate and the plenum zone. If the bolts are overtightened, the distributor plate deforms the lexan below it and restricts the brass-plug movement.

5.1.3.2 Mounting the Sliding Plug

Approximately 1 meter of 0.356-mm diameter wire was attached to each end of the sliding brass-plug. The plug was slid into the plenum zone of the cold-flow model. The wire on each end of the plug was then fed through a Swagelok fitting containing the O-ring, one for each end of the base section. These fittings were then screwed into the base section and sealed using silicone rubber.

The wire was threaded up through the brass tubing and the flexible metal hose using a large-diameter guide wire. The plug wire finally exits the 1/4-inch brass tubing at a vertical 1/4-inch to 1/2-inch reducing union. This union serves as the lower resting stop of the plunger when it is de-energized . At this point, the sliding plug could be drawn back and forth freely by hand in the plenum zone.

The plug was next pulled tight against the left end of the plenum zone and the wire was fed through the eyelet of the left plunger. Approximately 57.2 mm of wire must be between the lower resting stop and the bottom of the left-hand plunger. The actual full length movement of the plug is 50.8 mm. The additional length of wire insures that the de-energized solenoid will not prevent the sliding plug from seating. The wire on this side was twisted around itself securing the left-hand plunger.

The left-hand solenoid, a 12.7-mm O.D. tube with a coil wound on it, was then lowered over the left-hand plunger and secured to the reducing union. The sliding plug was drawn to the right end of the plenum by hand and the operation was repeated.

Following the orientation of both the left- and right-hand solenoids, plunger stops were inserted down into the magnetic-field region of each solenoid. These plunger stops were held in place using a 1/2-inch bored through Swagelok union and nylon ferrules. Initially, these stops were only roughly adjusted.

The system was pressure-tested by closing the outlet needle valve and pressurizing the system to a pressure of 170 kPa absolute (about 25 psia). The system was then returned to atmospheric pressure and sealing of the "plug seat," where the sliding plug comes in contact with the O-ring, was checked. If gas was leaking across the plug seat when the respective feed line was pressurized to 170 kPa absolute, the plunger stop was raised somewhat. This, in turn, caused more tension in the wire connecting the plunger and the plug, and more force against the plug seat.

At the conclusion of the above procedure, the cold-flow model was ready for gas-mixing or differential-pressure experiments.

5.1.3.3 Feed Gas Flow Rates

Feed-gas flow rates were set using the needle valves located just downstream of solenoid valves 1 and 2 in Figure 5.1. Again a critical pressure drop was maintained across these needle valves, making the flow rate independent of the downstream system pressure. Typically, the pressure upstream of solenoid valves 1 and 2 was maintained at 274.8 kPa (gauge) and the downstream pressure at 34.0 kPa (gauge).

The argon flow rate was set by first activating solenoid valve L, causing the sliding plug to seal against the left-hand plug seat. Pressure tap A (see Figure 5.1) was then opened and a bubble meter was connected to it using tygon tubing. Solenoid valve 1 (shown in Figure 5.1) was opened and the associated needle valve was adjusted to allow the desired flow rate of argon. This procedure was repeated in the helium feed-line.

The flow rate of feed gas used in the steady-state F-T synthesis experiments in the hot vibrofluidized-bed microreactor system was 3,670 standard mm^3 per second. This flow rate corresponds to a flow rate at conditions (395°C, 2,220 kPa absolute) of approximately 409 actual mm^3 per second. Feed-gas flow rates of argon and helium used in the cold flow model exprinents were maintained at approximating 417 actual mm^3 per second in order to duplicate the velocity in the hot rig.

5.1.3.4 Gas-Mixing Studies

Experiments were performed in the cold-flow model of the sliding-plug virbofluidized-bed microreactor in order to determine the extent of gas mixing in the three zones of the microreactor after switching from one feed gas to the other. For example, the gas-mixing properties of the plenum zone can be determined by first inserting the capillary sample tube into the base section of the model. The top of the capillary was inserted so that it was flush with the plenum zone wall and did not interfere with the movement of the sliding-plug. The nitrogen flow to the thermal conductivity detector was started at 1,170 standard mm^3 per second and the detector temperature and sensitivity were set to 100°C and 2, respectively. Helium and argon were allowed to flow into the gas reservoirs located upstream of solenoid valves 1 and 2 in Figure 5.1. These reservoirs were allowed to pressurize to 274.8 kPa (gauge). The remainder of the cold-flow model was then brought up to between 27 and 34 kPa (gauge) in the following fashion (refer to Figure 5.1). The exit-line needle valve was closed and the left solenoid (L) in the argon feed-line was actuated. This causes the sliding plug to move to the left end of the plenum zone. Solenoid valve 2 in the helium feed line was then opened, allowing helium to flow through the system. After two minutes of helium flow, solenoid valve 1 was opened and solenoid valve 2 was closed. At the same moment, the relay to the solenoids was switched causing solenoid L to de-energize, while solenoid R was energized. This drew the plug to the right-hand

end of the plenum. Argon was allowed to flow though the system for 2 minutes before flow of helium was resumed.

The switching procedure described above was continuously repeated using a microcomputer program, until the system reached the operating pressure. The exit-line needle valve was then opened slightly to allow the pressure to stabilize at the desired value. The microcomputer control continued switching the solenoid valves and the relay, while a thermal conductivity trace was obtained on the chart recorder.

The above procedure was repeated with the capillary sampling tube .inserted into the catalyst zone and the gas-exit zone of the cold-flow model. In addition, several feed-gas flow rates were used. The effect of catalyst vibrofluidization on gas mixing was investigated by vibrating the cold-flow model at a frequency of 13 to 24 Hertz (Hz) and a peak-to-peak amplitude of 4 mm.

Finally, a method of feed-gas flow staggering was devised. Staggering involves opening the opposite solenoid valve several seconds before the plug slides, thus allowing feed-gas valve openings to overlap somewhat. This causes the gas pressure to build up behind the plug seat. When the plug is moved to the opposite seat, the gas pressure rapidly sweeps the plenum zone.

5.1.3.5 Differential-Pressure Studies

Experiments were conducted in the cold-flow model in order to identify pressure buildup and pressure drop characteristics of the sliding-plug microreactor system. The procedure for these studies typically involved connecting a fast-response pressure transducer

(0 to 100 torr) between two pressure taps and then starting the feed-gas cycling. For example, a pressure-drop experiment·involved connecting the high-pressure inlet of the transducer to pressure tap A (shown in Figure 5.1) and the low-pressure inlet to the tap in the center of the catalyst section of the cold-flow model. This effectively placed the differential-pressure transducer across the distributor plate. The output of this fast-response transducer was connected to the storage oscilloscope and a digital multimeter. The system was pressurized in the manner described in Section 5.1.3.4 and the microcomputer initiated the feed-gas cycling. Using this rapid-response differential-pressure transducer setup, both steady-state and transient pressures could be recorded. Thus, pressure changes during plug movement could be monitored.

5.2 Experimental Results and Discussion

The objective of the cold-flow experiments in the sliding-plug vibrofluidized-bed microreactor model was to determine the gas-mixing properties of the microreactor upon rapid switching between two feed gases. In addition, it was desired to optimize the microreactor design so as to obtain rapid replacement of gas in the plenum zone and subsequently in the catalyst zone.

Experiments were performed using two distributor plates of different porosities, the second being chosen using information obtained with the first plate in the microreactor. Rapid-response differential-pressure measurements were used as the primary tool for the selection of distributor plates.

After choosing an appropriate distributor plate, the effects of vibrofluidization, feed-gas flow rate, and feed-gas staggering on gas mixing in the three zones (i.e., the plenum zone, the catalyst zone and the gas-exit zone) of the cold-flow microreactor model were explored.

Table 5.1 summarizes the experimental conditions and results for the cold-flow model studies. Each experiment is designated by a series number followed by an experiment number. Series 1 involved the use of a 20-micron distributor plate with the gas-sampling point located in the plenum zone of the model. Series 2, 3, and 4 all involved using a 2-micron distributor plate with the sampling point in the plenum zone, catalyst zone and gas-exit zone, respectively. Strip-chart recorder traces of the thermal conductivity detector output for all of these experiments are located in Appendix F.

5.2.1 Baseline Gas-Mixing Information

In order to determine the minimum observable transition time when switching from argon to helium and from helium to argon, a series of baseline experiments were performed. These experiments involved replacing the cold-flow microreactor model with a manual 3-way ball valve. The remainder of the system was not altered. The capillary sampling tube was placed so that its tip extended directly into the center of the ball valve, as shown schematically in Figure 5.7. The system pressure was maintained at 37.2 kPa and the flow rates were set at 417, 833 and 1650 actual mm^3/sec for the three experiments. Thermal conductivity detector settings were those specified in Section 5.1.3.

TABLE 5.1

Experimental Conditions and Results for the Cold-Flow Model Studies

Experiment Number	Plate Grade (μ)		Feed-Gas Flow Rate (actual mm^3/s)		System Pressure (kPa)	Capillary Sampling Position	Catalyst Vibrofluidized
	Distributor	Catalyst Retention	Helium	Argon			
1-1	20	40	435	435	38.5	Plenum	No
1-2	20	40	435	435	31.3	Plenum	No
1-3	20	40	435	435	31.3	Plenum	No
1-4	20	40	435	435	36.5	Plenum	No
1-5	20	40	435	435	36.5	Plenum	No
1-6	20	40	435	435	36.5	Plenum	No
1-7	20	40	435	435	36.5	Plenum	No
1-8	20	40	435	435	31.6	Plenum	No
1-9	20	40	417	417	38.2	Plenum	No
1-10	20	20	417	417	33.8	Plenum	No

TABLE 5.1 (Continued)

Experiment Number	Feed-Gas Staggering (s)	Fast Response ΔP Measurement	ΔP Transducer Connections	Chart Speed (cm/min)	Recent Full-Scale Transition After 2.4 seconds (%)	
					He-to-Ar Transition	Ar-to-He Transition
1-1	No	No	-	2	93.7	71.3
1-2	No	Yes	Tap A to Catalyst Zone	2	-	-
1-3	Yes, 5	Yes	Tap A to Catalyst Zone	2	95.1	87.9
1-4	No	Yes	Tap A to Tap B	2	91.8	69.6
1-5	Yes, 5	Yes	Tap A to Tap B	2	96.2	86.6
1-6	Yes, 5	Yes	Tap B to Catalyst Zone	2	96.1	87.2
1-7	No	Yes	Tap B to Catalyst Zone	2	91.6	72.3
1-8	No	Yes	Tap A to Catalyst Zone	2	92.4	69.0
1-9	No	Yes	Tap A to Tap B	2	86.2	-
1-10	No	No	-	2, 10	89.4	75.6

TABLE 5.1 (Continued)

Experiment Number	Plate Grade (μ)		Feed-Gas Flow Rate (actual mm³/s)		System Pressure (kPa)	Capillary Sampling Position	Catalyst Vibrofluidized
	Distributor	Catalyst Retention	Helium	Argon			
2-1	2	20	417	417	27.1	Plenum	No
2-2	2	20	417	417	33.5	Plenum	No
2-3	2	20	800	800	31.8	Plenum	No
2-4	2	20	417	417	31.8	Plenum	Yes
2-5	2	20	417	417	31.8	Plenum	Yes
2-6	2	20	417	417	31.8	Plenum	No
2-7	2	20	417	417	31.8	Plenum	No
2-8	2	20	417	417	33.8	Plenum	No
2-9	2	20	417	417	33.8	Plenum	No
2-10	2	20	833	833	34.5	Plenum	No
2-11	2	20	833	833	34.5	Plenum	No
2-12	2	20	1650	1650	38.2	Plenum	No
2-13	2	20	1650	1650	36.5	Plenum	No

TABLE 5.1 (Continued)

Experiment Number	Feed-Gas Staggering (s)	Fast Response ΔP Measurement	ΔP Transducer Connections	Chart Speed (cm/min)	Percent Full-Scale Transition After 2.4 seconds (%)	
					He-to-Ar Transition	Ar-to-He Transition
2-1	No	No	-	2	95.6	88.7
2-2	No	No	-	2, 10	97.1	90.2
2-3	No	No	-	2, 10	96.9	93.2
2-4	Yes, 2	No	-	2	-	-
2-5	Yes, 5	No	-	2	-	-
2-6	Yes, 2	No	-	2, 10	96.8	93.6
2-7	Yes, 5	No	-	2, 10	97.1	95.7
2-8	No	Yes	Tap A to Catalyst Zone	2	95.9	91.1
2-9	No	Yes	Tap B to Catalyst Zone	2	97.0	89.8
2-10	No	No	-	10	97.0	93.9
2-11	Yes, 5	No	-	10	97.8	97.8
2-12	No	No	-	10	99.4	96.2
2-13	Yes, 5	No	-	10	99.5	99.1

TABLE 5.1 (Continued)

Experiment Number	Plate Grade (μ)		Feed-Gas Flow Rate (actual mm^3/s)		System Pressure (kPa)	Capillary Sampling Position	Catalyst Vibrofluidized
	Distributor	Catalyst Retention	Helium	Argon			
3-1	2	20	417	417	31.8	Catalyst Zone	No
3-2	2	20	417	417	31.8	Catalyst Zone	Yes
3-3	2	20	417	417	31.8	Catalyst Zone	No
3-4	2	20	417	417	36.9	Catalyst Zone	Yes
3-5	2	20	850	850	32.8	Catalyst Zone	No
3-6	2	20	850	850	35.5	Catalyst Zone	Yes
3-7	2	20	850	850	35.5	Catalyst Zone	No
3-8	2	20	850	850	35.5	Catalyst Zone	Yes
3-9	2	20	1650	1650	29.8	Catalyst Zone	No
3-10	2	20	1650	1650	30.8	Catalyst Zone	Yes
3-11	2	20	1650	1650	30.8	Catalyst Zone	No
3-12	2	20	1650	1650	30.8	Catalyst Zone	Yes

TABLE 5.1 (Continued)

Experiment Number	Feed-Gas Staggering (s)	Fast Response ΔP Measurement	ΔP Transducer Connections	Chart Speed (cm/min)	Percent Full-Scale Transition After 2.4 seconds (%)	
					He-to-Ar Transition	Ar-to-He Transition
3-1	No	No	-	2, 10	89.6	63.0
3-2	No	No	-	2, 10	83.3	60.2
3-3	Yes, 5	No	-	2, 10	95.6	89.4
3-4	Yes, 5	No	-	2, 10	93.6	77.3
3-5	No	No	-	2, 10	92.6	81.1
3-6	No	No	-	2, 10	84.1	73.0
3-7	Yes, 5	No	-	2, 10	97.3	93.8
3-8	Yes, 5	No	-	2, 10	96.7	93.4
3-9	No	No	-	2, 10	97.0	91.0
3-10	No	No	-	2, 10	90.6	88.0
3-11	Yes, 5	No	-	2, 10	97.3	97.3
3-12	Yes, 5	No	-	10	97.3	97.3

TABLE 5.1 (Continued)

| Experiment Number | Plate Grade (μ) | | Feed-Gas Flow Rate (actual mm^3/s) | | System Pressure (kPa) | Capillary Sampling Position | Catalyst Vibrofluidized |
	Distributor	Catalyst Retention	Helium	Argon			
4-1	2	20	417	417	38.9	Exit Zone	No
4-2	2	20	417	417	37.9	Exit Zone	Yes
4-3	2	20	417	417	37.9	Exit Zone	No
4-4	2	20	417	417	37.9	Exit Zone	Yes
4-5	2	20	833	833	37.6	Exit Zone	No
4-6	2	20	833	833	37.6	Exit Zone	Yes
4-7	2	20	833	833	39.3	Exit Zone	No
4-8	2	20	833	833	39.3	Exit Zone	Yes
4-9	2	20	1650	1650	32.1	Exit Zone	No
4-10	2	20	1650	1650	32.1	Exit Zone	Yes
4-11	2	20	1650	1650	34.9	Exit Zone	No
4-12	2	20	1650	1650	34.9	Exit Zone	Yes

TABLE 5.1 (Continued)

Experiment Number	Feed-Gas Staggering (s)	Fast Response ΔP Measurement	ΔP Transducer Connections	Chart Speed (cm/min)	Percent Full-Scale Transition After 2.4 seconds (%)	
					He-to-Ar Transition	Ar-to-He Transition
4-1	No	No	-	2, 10	78.7	42.5
4-2	No	No	-	2, 10	79.7	42.4
4-3	Yes, 5	No	-	2, 10	93.0	74.1
4-4	Yes, 5	No	-	2, 10	90.8	67.2
4-5	No	No	-	2, 10	83.5	61.0
4-6	No	No	-	2, 10	83.3	54.7
4-7	Yes, 5	No	-	2, 10	97.5	88.2
4-8	Yes, 5	No	-	2, 10	96.6	86.8
4-9	No	No	-	2, 10	96.2	75.9
4-10	No	No	-	2, 10	91.7	73.0
4-11	Yes, 5	No	-	2, 10	98.6	92.8
4-12	Yes, 5	No	-	2, 10	98.1	95.1

capillary to TCD

to downstream system

Ar feed line

He feed line
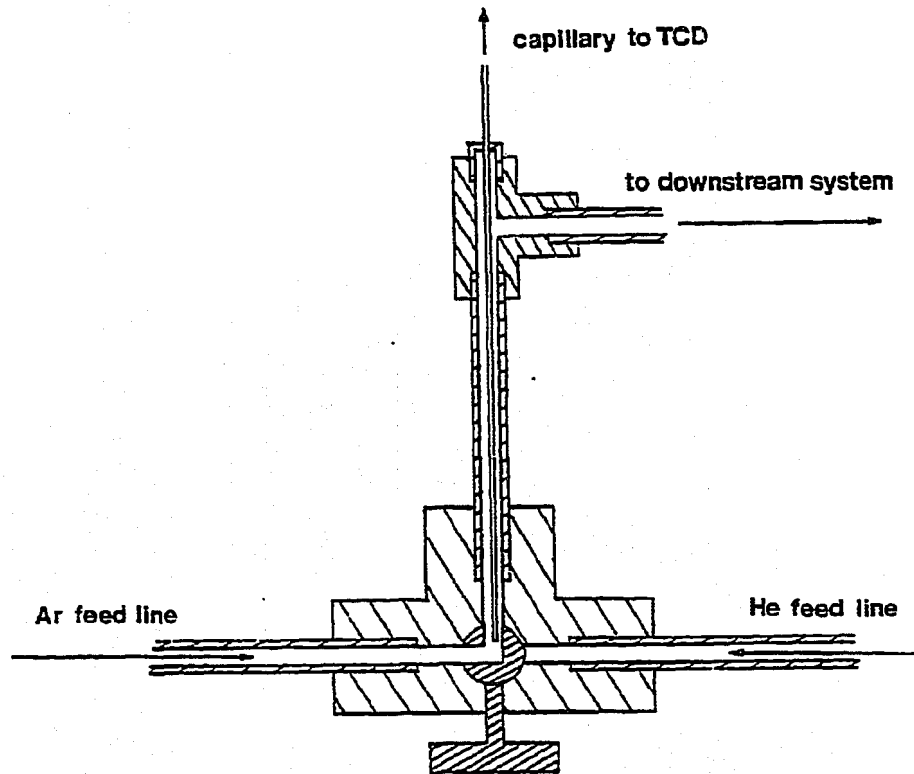
Figure 5.7. A Schematic Diagram of the Manual 3-way
Valve Setup for Baseline Gas-Mixing
Information.

In sum, the system equipment and variables were the same as those used throughout the cold-flow model experiments with the exception of the replacement of the sliding-plug microreactor by a 3-way manual valve.

The procedure for this experiment involved rapidly turning the 3-way valve in synchronization with the computer switching of the solenoid valve. Figure 5.8 is the TCD (thermal conductivity detector) response for switching between helium and argon feeds at 417 actual mm^3 per second.

As shown in Figure 5.8, the upper plateau is the argon baseline, while the lower plateau is the helium baseline. At 77°C, the thermal conductivities of helium, argon and nitrogen are 0.166, 0.0200 and 0.0293 W/m-K, Therefore, the pure nitrogen baseline lies between the baseline of the argon-nitrogen mixture (upper baseline) and the helium-nitrogen mixture (lower baseline). These gas mixtures are produced when the gas being sampled via the capillary bleeds into the nitrogen carrier gas stream going to the TCD.

Figures 5.9 and 5.10 are similar TCD outputs for flow rates of 833 and 1650 actual mm^3 per second. The time for a 100% transition from the argon baseline to the helium baseline as well as from the helium baseline to the argon baseline is approximately 2.4 seconds.

Comparing Figures 5.8, 5.9, and 5.10, it can be seen that this transition time is unaffected by feed-gas flow rates. This indicates that the gas sampling and detection system introduces a very small amount of gas mixing. This mixing could possibly be introduced at the
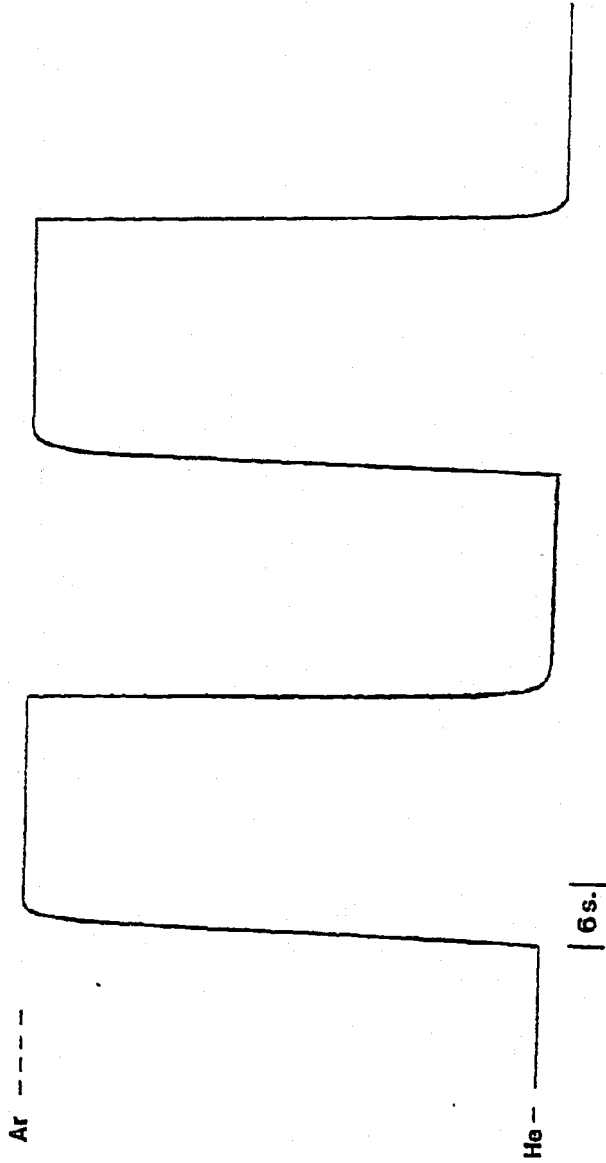
Figure 5.8. The TCD Response for Switching Between Helium and Argon Feeds at 417 Actual mm3/s Substituting a Manual 3-Way Valve for the Microreactor. (Ar=Argon baseline, He= Helium baseline).
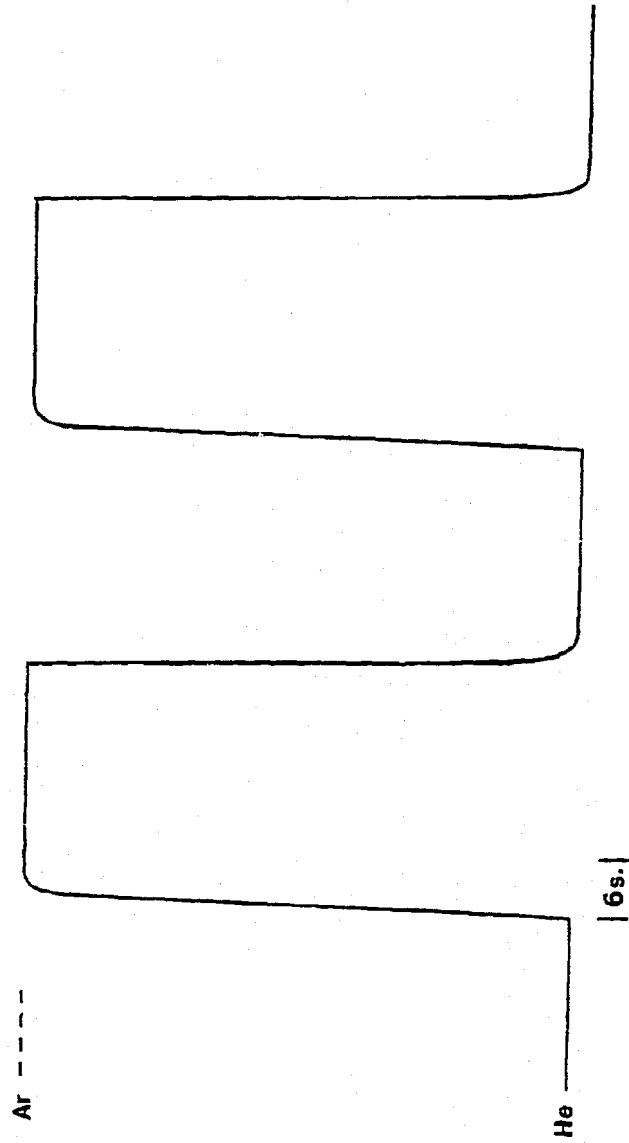
Figure 5.9. The TCD Response for Switching Between Helium and Argon Feeds at 833 Actual mm^3/d Substituting a Manual 3-Way Valve for the Micro-reactor (Ar=Argon baseline, He=Helium baseline).
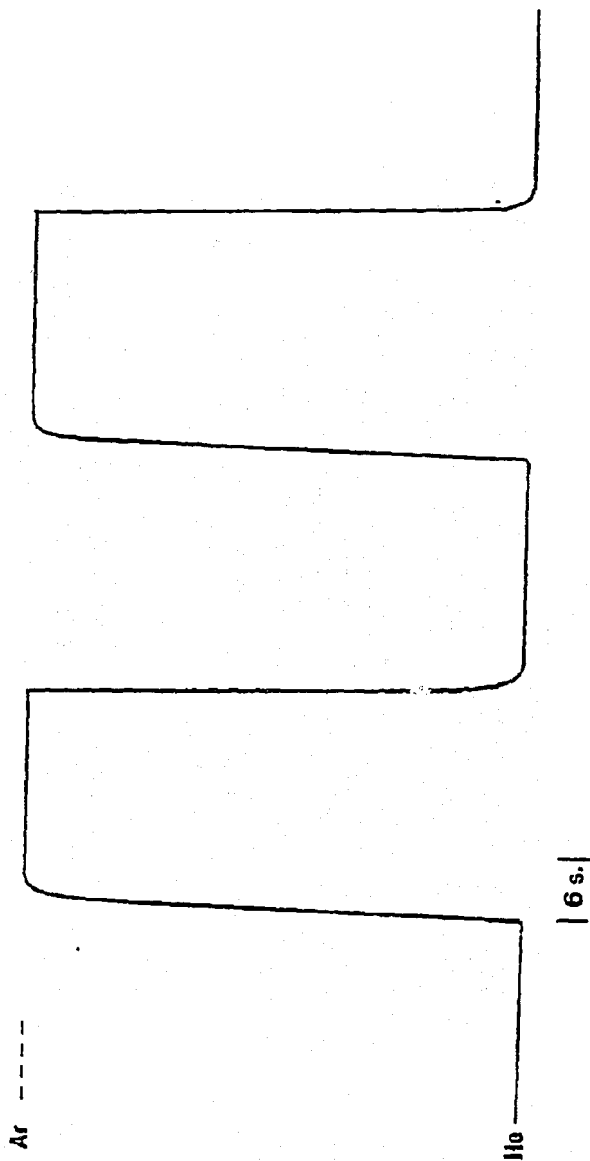
Figure 5.10. The TCD Response for Switching Between Helium and Argon Feeds at 1650 Actual mm3/s Substituting a Manual 3-Way Valve for the Micro-reactor (Ar=Argon baseline, He=Helium baseline).

point where the capillary tubing bleeds argon or helium into the
nitrogen carrier gas stream (refer to Figure 5.1). In addition, mixing
could be induced by the flow path through the thermal conductivity cell
in the detector. At any rate, the shortest possible transition time for
100% change in the feed gas is 2.4 seconds for the gas sampling and
detection system. Therefore, a transition time of 2.4 seconds has been
used as a reference for gas-mixing transitions throughout this study.

5.2.2 Cold-Flow Model Gas-Mixing Experiments Using a 20-Micron Distributor Plate

Preliminary experiments (Experiments 1-1 through 1-10) were
undertaken in the cold-flow sliding-plug vibrofluidized-bed microreactor
model with a 20-micron distributor plate at feed-gas flow rates in
the range of 435 actual mm^3 per second.

Figure 5.11 (Experiment 1-10) shows the TCD output for gas mixing
in the plenum zone of the cold-flow model. The helium-to-argon
transition shows that 89.4% of the helium in the plenum has been
replaced by argon after 2.4 seconds. However, the trace indicates a
slight hysteresis effect, followed by a slow transition to the argon
baseline.

The argon-to-helium transition shows a similar but more pronounced
effect as that described above. Initially, only 75.6% of the argon in
the plenum is replaced by helium after 2.4 seconds. Following the
rather rapid, initial 2.4-second transition, it takes approximately one
minute for the new feed gas to completely purge the old gas in the
plenum. This hysteresis or rebound effect and the slow transition are

Ar Baseline – – –

He Baseline . – – –
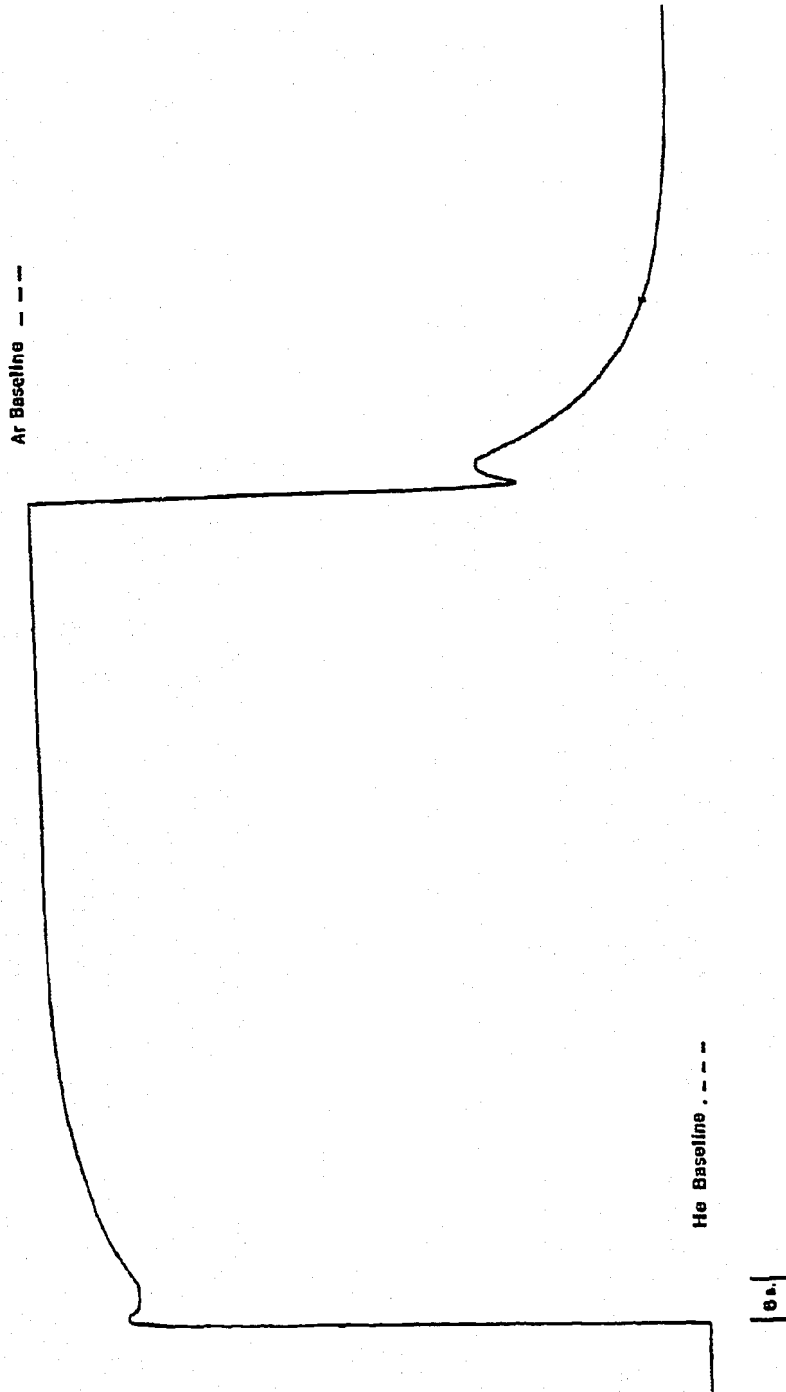
Figure 5.11. The TCD Response for Switching Between Helium and Argon Feeds at 417 Actual mm3/s in the Cold-Flow Microreactor Model with a 20-Micron Distributor Plate (see Experiment 1-10 in Table 5.1 for Experimental Conditions).

signs of incomplete gas removal in the plenum zone. In order to explain the rebound and slow transition, two theories were developed and tested: (1) the backflow theory; and (2) the annular-flow theory.

5.2.2.1 Backflow Theory

In principle, there should be no mixing of feed gases in the plenum zone upon sliding of the plug. The plug should effectively "pump out" and compress the previous feed gas, while simultaneously drawing in the new feed gas. This should cause a discrete transition in feed gases in the plenum. However, this is not the case (as shown in Figure 5.11).

The theory of backflow speculates that a region of high pressure is created in the catalyst zone by the sliding plug, while a region of low pressure develops behind the plug as it moves. If the distributor plate is too porous, gas in front of the plug is compressed into the catalyst zone as well as the feed-gas line, as the plug slides. Behind the plug, the increased volume of the space causes the pressure to drop. As the plug approaches the end of its stroke, high-pressure gas from the catalyst zone (gas A) backflows through the porous plate into the lower-pressure plenum zone containing the new feed gas (gas B). This backflow results in gas mixing in the plenum zone.

In order to test this theory, plug-velocity and rapid-response differential-pressure measurements were made. The velocity of the plug was measured using a circuit shown in Figure 5.12. When the plug is in contact with either end stop, the output from the circuit is +28 VDC. As soon as the plug begins to move, it breaks contact with the stop and the circuit output falls to ground potential. When the plug contacts
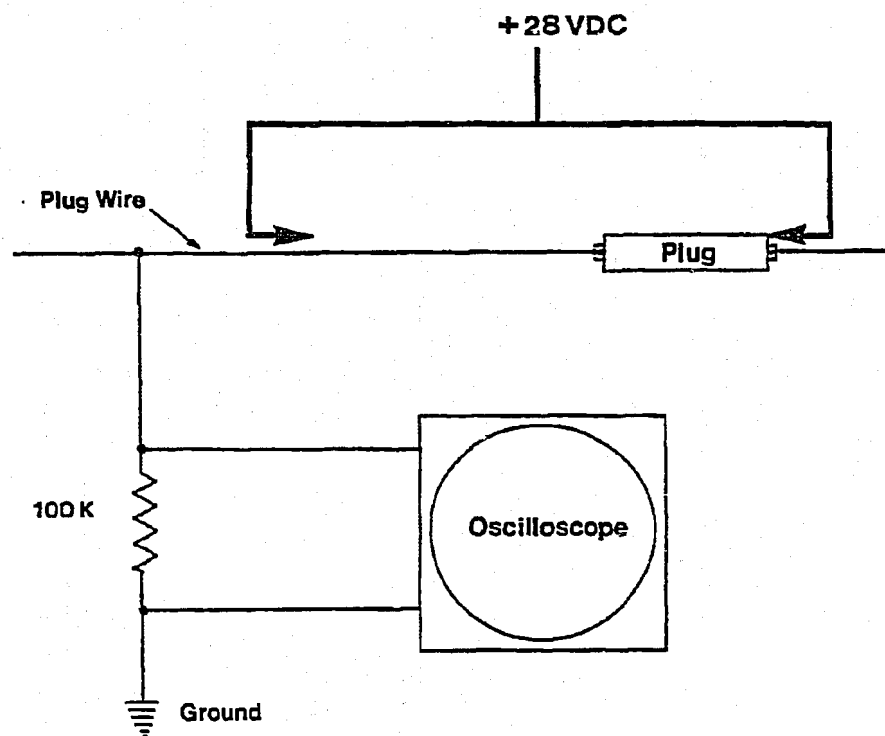
Figure 5.12. A Schematic of the Plug-Velocity
Measurement Circuit.

the other plug stop, the potential again rises to +28 VDC. The output
is recorded as a square-wave valley on the oscilloscope. The plug was
found to move 50.8 mm in 65 msec, resulting in a velocity of 0.78 m/sec.
At this velocity, no significant velocity head is developed. This
result indicates that the drop in pressure behind the plug is mainly
caused by the effective increased volume of the feed line.

Rapid-response differential-pressure measurements consisted of
experiments with the transducer in three different positions.

1. Experiments 1-2, 1-3, and 1-8 involved connecting the
transducer between tap A (see Figure 5.1) in the argon feed-line and the
catalyst zone.

2. Experiments 1-6 and 1-7 involved connecting the transducer
between tap B (see Figure 5.1) in the helium feed-line and the catalyst
zone.

3. Finally, experiments 1-4, 1-5, and 1-9 involved connecting the
differential-pressure transducer between tap A in the argon feed-line
and tap B in the helium feed-line.

Experiments 1-2 through 1-7 were performed using a 10-torr
rapid-response differential-pressure transducer. This transducer has
been calibrated to a range of ±4.98 kPa, at which point it saturates
producing a constant output. Experiments 1-8 and 1-9, however, were
performed using a 100-torr rapid-response differential-pressure
transducer. Therefore, these latter experiments had a linear range
between ±13.1 kPa. Figure 5.13 is an oscilloscope trace for the
helium-to-argon and argon-to-helium transitions during Experiment 1-2.
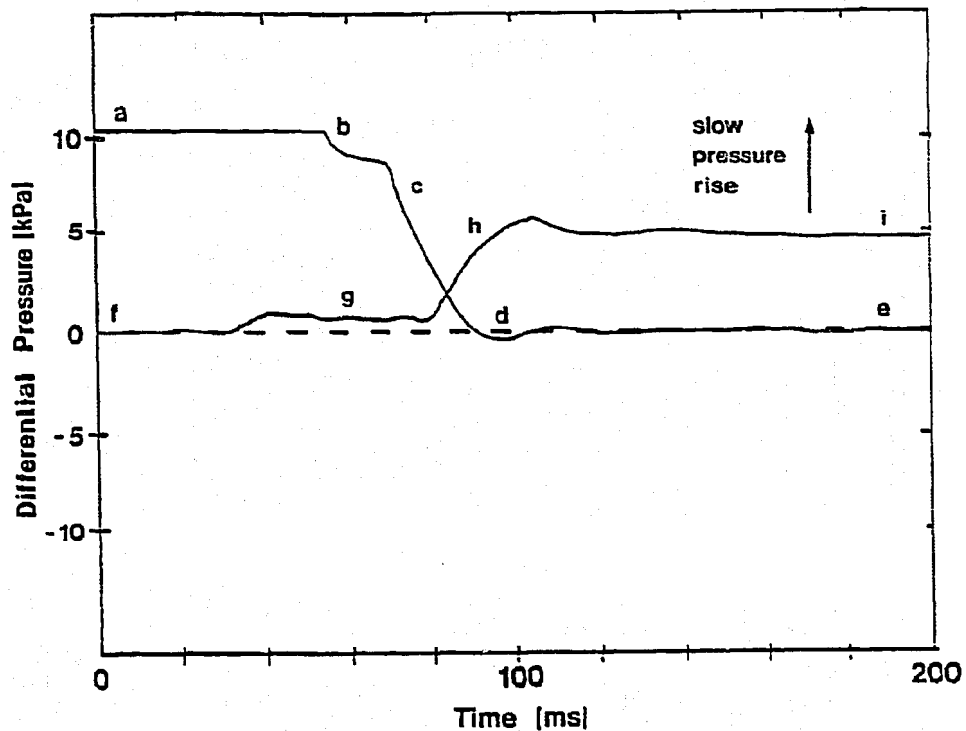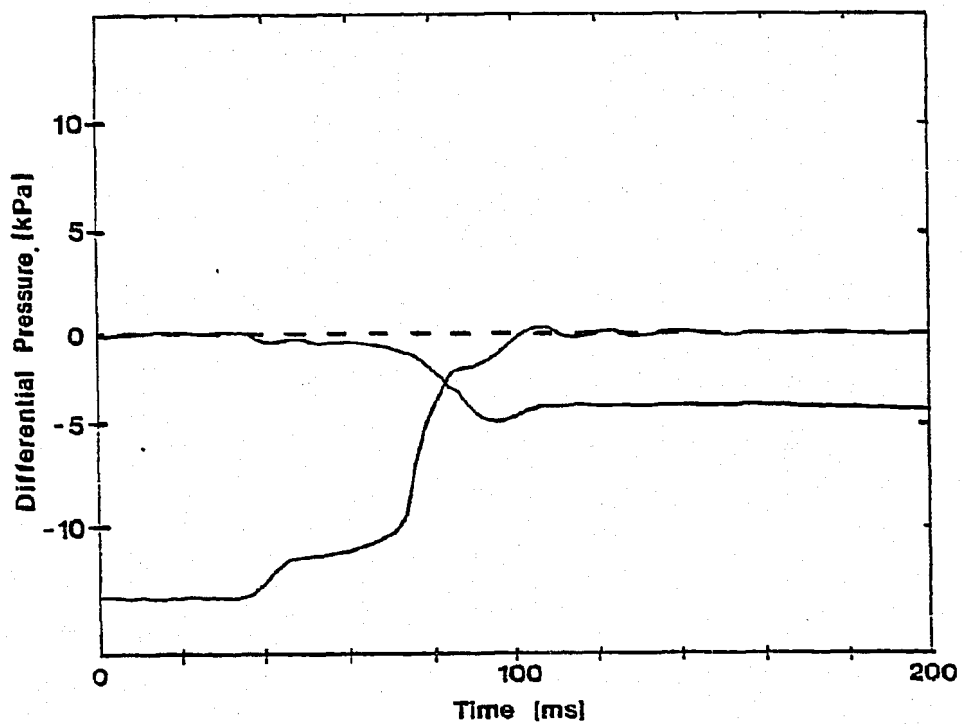
Figure 5.13. An Oscilloscope Trace from a Differential-
Pressure Transducer Placed Between the
Argon Feed-Line (Tap A in Figure 5.1) and
the Catalyst Zone. The Oscilloscope
Triggered at the Beginning of Plug Move-
ment. See Text for Explanations of Points
a to i. (Experiment 1-2 in Table 5.1).

Referring to the system diagram shown in Figure 5.1, the following sequence of events indicating the pressure behavior during plug movement has been pieced together.

1. Point "a": The plug is against the left-hand stop. Helium is being fed through the microreactor and argon is stagnant in its feed-line. The pressure in the argon feed-line is greater than that in the catalyst zone, because argon has been compressed into its feed-line by the previous plug transition. The transducer is saturated at this point.

2. Point "b": The plug has begun to move away from the left-hand stop and toward the right-hand stop. As soon as the plug begins moving, solenoid valve 1 is opened, while 2 is closed.

3. Point "c": The plug is approximately in the middle of its stroke. The pressure difference between the argon feed-line and the catalyst zone drops. Gas is compressed into the heliuim feed-line and the catalyst zone.

4. Point "d": The plug is at the end of its stroke, at the righ-hand stop. The pressure in the catalyst zone is greater than that in the argon feed-line.

5. Point "e": Argon is now being fed to the microreactor and the pressures in the argon feed-line and the catalyst zone have equalized.

6. Point "f": Similar to point "e". Argon is being fed and helium is stagnant behind the plug.

7. Point "g": The plug has started moving from right to left. The pressure in the argon feed-line builds up slightly and levels off for 40

ms. This is due to simultaneous buildup of pressure in the catalyst zone as well. Therefore, the differential pressure stabilizes for approximately 40 ms.

8. Point "h": The plug-end has past the left end of the distributor plate. In this region, gas is being compressed into the argon feed-line only. Therefore, the differential pressure between the argon feed-line and the catalyst zone builds up rapidly.

9. Point "i": The pressure difference between the stagnant argon feed-line and the catalyst zone containing flowing helium has stabilized somewhat. The differential pressure continues to increase, because of pressure buildup in the argon feed-line due to a phenomenon called "bleed-down." Briefly, "bleed-down" is the transfer of high-pressure gas trapped between the feed-line solenoid valve and needle valve after the solenoid valve closes. The pressure increases until the transducer saturates producing a pressure level identical to that of point "a".

Figure 5.14 is a similar oscilloscope trace taken in Experiment 1-7. During this experiment, the rapid-response differential-pressure transducer was placed between tap B in the helium feed-line and the catalyst zone. This trace is a near identical mirror-image of Figure 5.13, indicating similar pressure behavior in the helium feed-line and the argon feed-line.

The most interesting point shown in Figures 5.13 and 5.14 is the time period when the pressure in the catalyst zone becomes greater than that in the feed line. For this short period of time, gas actually
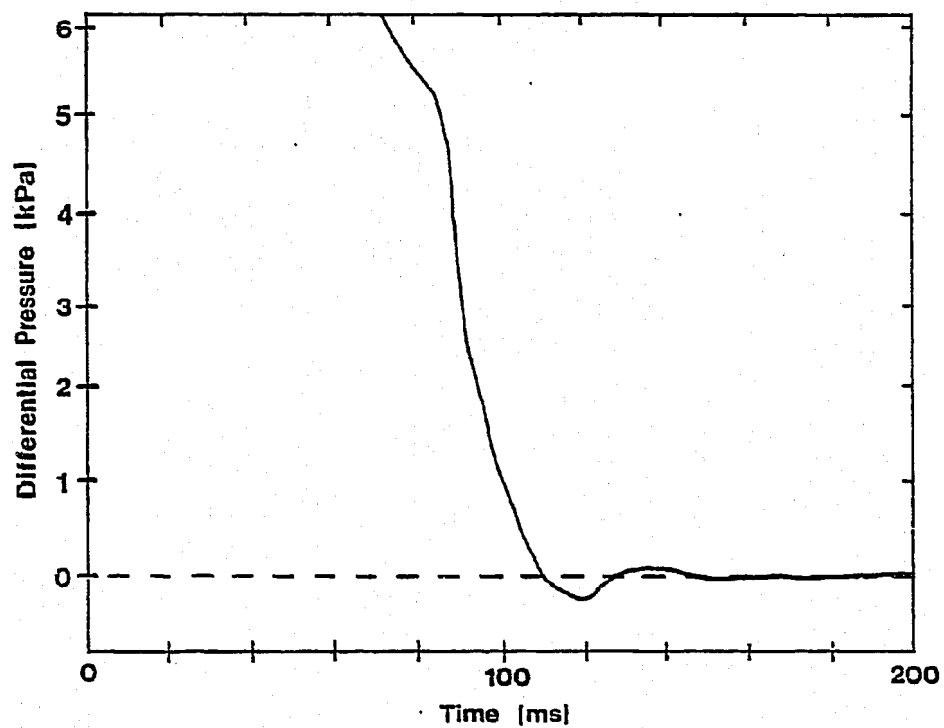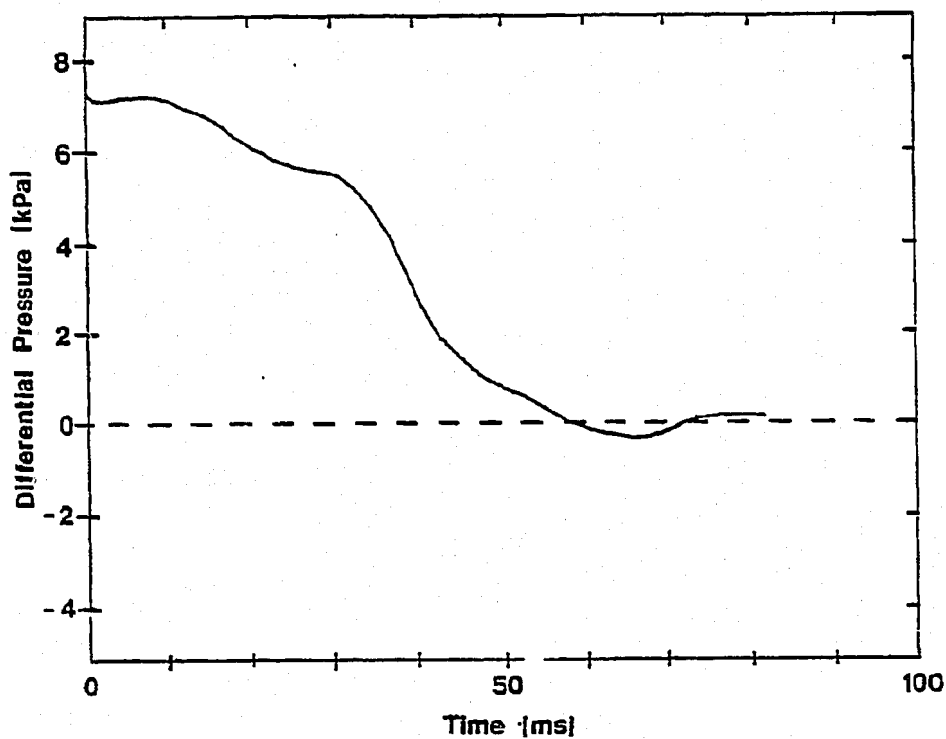
Figure 5.14. An Oscilloscope Trace from a Differential-Pressure Transducer Placed Between the Helium Feed-Line (Tap B in Figure 5.1) and the Catalyst Zone. The Oscilloscope Triggered at the Beginning of Plug Movement. (Experiment 1-7 in Table 5.1).

backflows from the catalyst zone through the distributor plate into the plenum zone. Experiment 1-7 was performed in order to determine the magnitude and duration of this pressure inversion. Figures 5.15 and 5.16 illustrate the results of this experiment. The pressure inversion lasts 13 msec, and its magnitude is approximately 0.346 kPa. The total system pressure during the experiment was 36.5 kPa. Therefore, the pressure inversion was 0.95% of the total.

The volume of gas which can backflow across the 20μ distributor plate in 13 msec with a pressure inversion of 0.346 kPa can be calculated using the standard equation for pressure drop as a function of gas flow as provided by the sintered stainless-steel plate manufacturer. This calculation is presented in Appendix A. It was determined that the possible volume of gas backflowing during the pressure inversion period is approximately 126.4 mm^3 of argon during the argon-to-helium transition and 1447.5 mm^3 of helium during the helium-to-argon transition. This corresponds to 8% and 90% of the plenum volume, respectively.

Calculations were performed for 5-, 2- and 0.5-micron distributor plates assuming the same magnitude and duration of pressure inversion. It was found that the theoretical backflow volume was reduced greatly on going to less porous distributors. Indeed, it seemed possible that backflow could be eliminated all together during the sliding-plug movement if the distributor-plate pressure drop was high enough to force gas compression in the feed line rather than the catalyst zone.
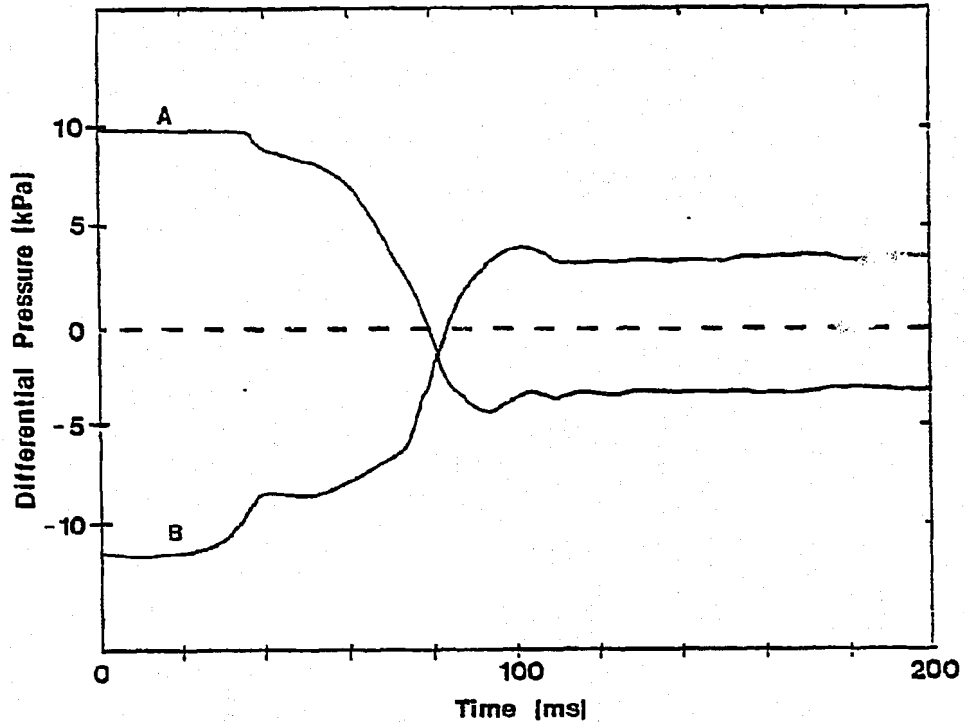
Figure 5.15. The Oscilloscope Trace from a Differen-
tial-Pressure Transducer Placed Between
the Argon Feed-Line (Tap A in Figure
5.1) and the Catalyst Zone. The Y Axis
Has Been Expanded and the Helium-to-Argon
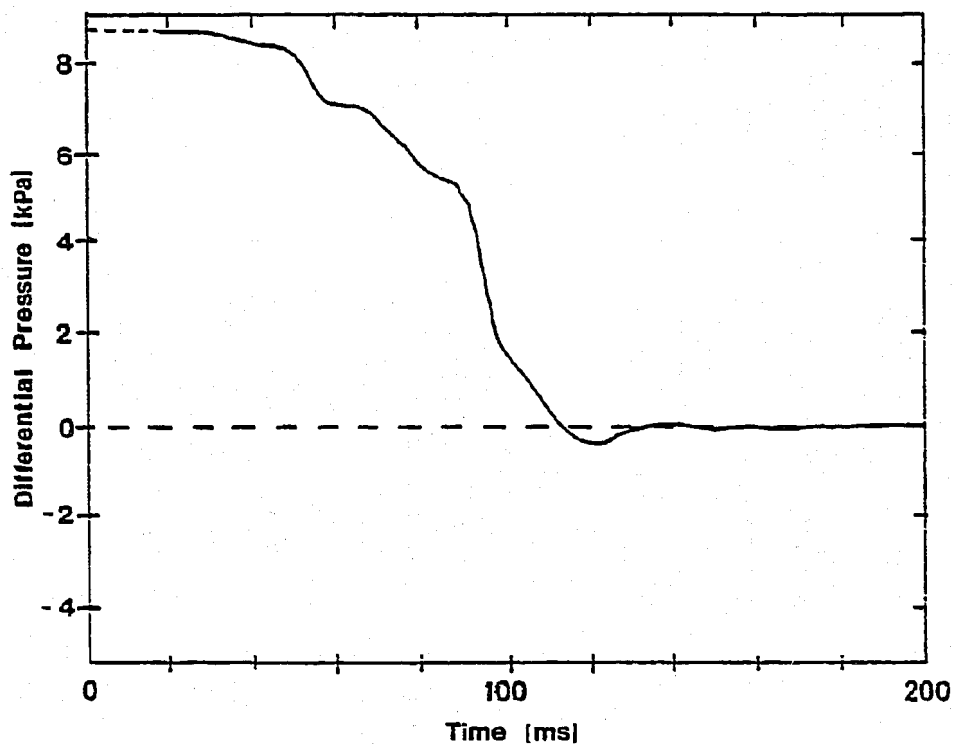Transition Is Shown. (Experiment 1-8
in Table 5.1).

Figure 5.16. The Oscilloscope Trace from a
Differential-Pressure Transducer
Placed Between the Argon Feed-Line
(Tap A in Figure 5.1) and the Catalyst
Zone. The Time Axis Has Been Expanded
and the Helium-to-Argon Transition Is
Shown. (Experiment 1-7 in Table 5.1).

Experiment 1-4 was performed in order to determine the differential pressure between the argon and helium feed-lines during plug movement. The 10 torr rapid-response differential-pressure transducer was connected between tap A in the argon feed-line and tap B in the helium feed-line. Figure 5.17 shows the transducer output for the transition from helium to argon feed (trace A) and from argon to helium feed (trace B). The differential pressures immediately following these transitions are shown in the time period of 120 to 200 ms. Using these initial differential pressures, the approximate amount of gas compressed from the plenum zone into the feed line could be determined. Using the system volumes specified earlier and the system pressure given in Table 5.1 for experiment 1-4, it was calculated that only 37% of argon feed gas was compressed back into the feed line.

Similarly, it was determined that during the helium-to-argon feed transition, only 33% of the helium feed gas was compressed into the helium feed-line. It follows that the remaining 63% and 67% of these gases are compressed into the catalyst zone, or are lost to annular flow around the sliding plug. Once the plug has reached the end of the plenum zone and sealed against the seat, the pressure in the sealed feed line slowly begins to build up due to the bleed-down phenomenon previously mentioned.

When a feed-gas solenoid valve is closed, a small amount of gas is trapped between the solenoid valve and the needle valve. The trapped gas, initially at the cylinder-regulator delivery pressure of 274.3 kPa, slowly bleeds across the needle valve into the stagnant feed-line,
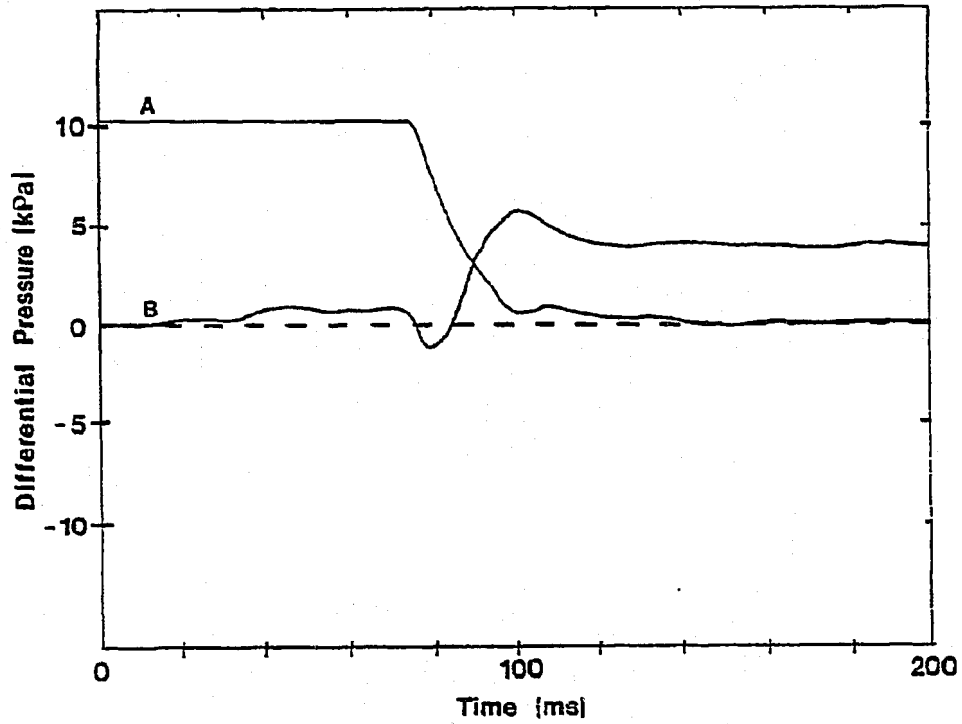
Figure 5.17. The Oscilloscope Trace from a Differential-Pressure Transducer Placed Between the Argon Feed Line (Tap A in Figure 5.1) and the Helium Feed-Line (Tap B in Figure 5.1). Curve A Is the Helium-to-Argon Transition and Curve B Is the Argon-to-Helium Transition. (Experiment 1-4 in Table 5.1).

causing the pressure in that line to build up. An example of the magnitude of this pressure buildup is illustrated by considering the stagnant argon feed-line. Immediately after the plug is switched and the argon flow is shut off, the pressure in the argon feed-line is 3.18 kPa. After 90 seconds of bleed-down, the pressure has more than doubled to 8.47 kPa as shown in Figure 5.18 (Experiment 1-8). The volume of argon added by bleed-down after 90 seconds is approximately 1,681 mm^3, coincidentally just slightly more than the volume displaced when the plug moves across the plenum zone (1,609 mm^3). During an actual synthesis experiment using a sliding-plug microreactor, the plug-switching period would be on the order of seconds rather than minutes and bleed-down would not play a significant role in pressure buildup.

A way of artifically eliminating backflow when using the 20-micron distribtor plate was also developed. Consider, for example, helium being fed to the microreactor and argon sitting stagnant behind the plug. Five seconds before the movement of the plug, solenoid valve 1 would be opened in the argon feed-line allowing pressure to build up behind the plug. During the subsequent plug movement, the pressure in the argon feed-line would not fall below that of the catalyst zone and backflow would not occur. The same procedure of premature Solenoid-valve opening would be repeated in the helium feed-line before the next plug transition. This method of pressure buildup behind the sliding plug is termed "Staggering." Five-second staggering implies that the feed-gas solenoid is opened 5 seconds before the plug is moved.
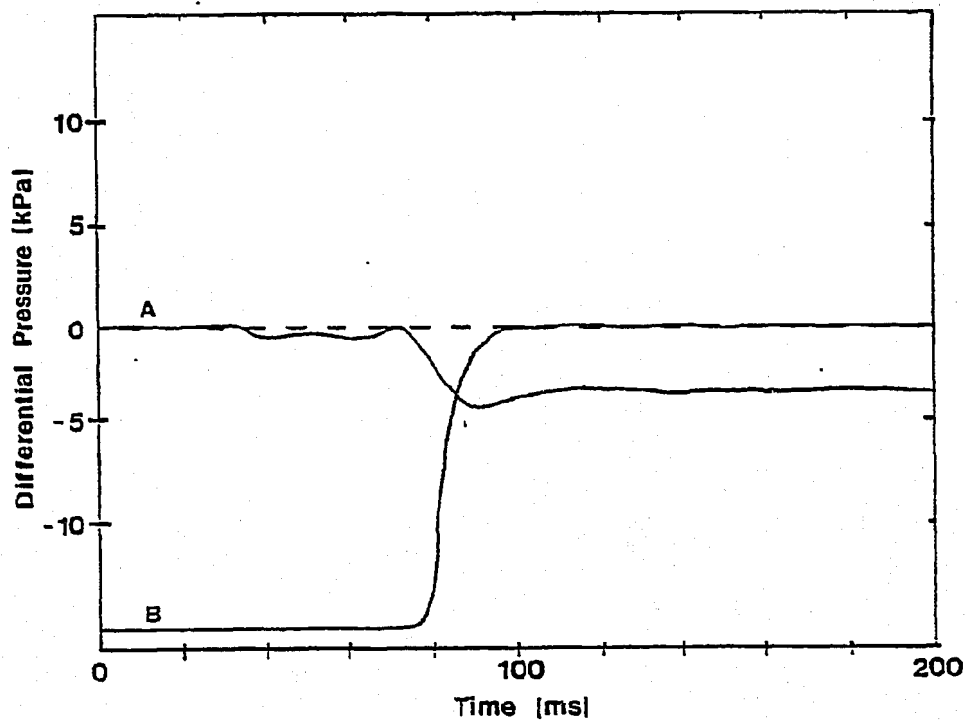
Figure 5.18. The Oscilloscope Trace from a
Differential-Pressure Transducer
Placed Between the Argon Feed-Line
(Tap A in Figure 5.1) and the
Catalyst Zone. The Y Axis Has Been
Expanded and the Helium-to-Argon
Transition Is Shown (Experiment 1-8
in Table 5.1).

Figures 5.19 and 5.20 show the results of 5-second staggering obtained in Experiments 1-5 and 1-6. The pressure inversion experienced in Figures 5.13 and 5.14 has been totally eliminated. Figure 5.21 is the TCD trace of gas mixing produced in the plenum during Experiment 1-3, in which 5-second staggering was used. Comparing these results to those of Experiment 1-10 with no staggering (Figure 5.11), a number of differences can be seen. Using staggering, the hysteresis effect has been greatly reduced. Where a spike appeared before, a plateau in now found. The percent change in gas in the plenum zone after 2.4 seconds has been increased from 89.4% to 95% for the helium-to-argon transition and from 75.6% to nearly 88% for the argon-to-helium transition.

5.2.2.2 Annular-Flow Theory

A second theory was developed to explain the cause of gas mixing in the plenum zone of the cold-flow sliding-plug vibrofluidized-bed microreactor model. It was speculated that when the plug was in transit, gas could be passing through the annular region between the plug and the plenum wall.

Experiment 1-9 was designed to test the validity of the annular flow theory. A diaphragm and the fast-response differential-pressure transducer were placed between taps A and B in the feed lines of the cold-flow model system. The diaphragm consisted of a Bellofram gauge protector, which is claimed to be able to respond to as little change as 0.249 kPa. The diaphragm inside the gauge protector is more flexible in one direction than the other due to the way it was manufactured. The more flexible side was connected to the argon feed-stream (tap A),

Figure 5.19. The Oscilloscope Trace from a Differential-
             Pressure Transducer Placed Between the
             Argon Feed-Line (Tap A in Figure 5.1)
             and the Catalyst Zone with 5-Second
             Staggering. (Experiment 1-5 in Table
             5.1). Curve A Is the Helium-to-Argon
             Transition and Curve B Is the Argon-to-
             Helium Transition.

Figure 5.20. The Oscilloscope Trace from a Differential-
Pressure Transducer Placed Between the
Helium Feed-Line (Tap B in Figure 5.1)
and the Catalyst Zone with 5-Second
Staggering. (Experiment 1-6 in Table
5.1). Curve A Is the Helium-to-Argon
Transition and Curve B Is the Argon-
to- Helium Transition.
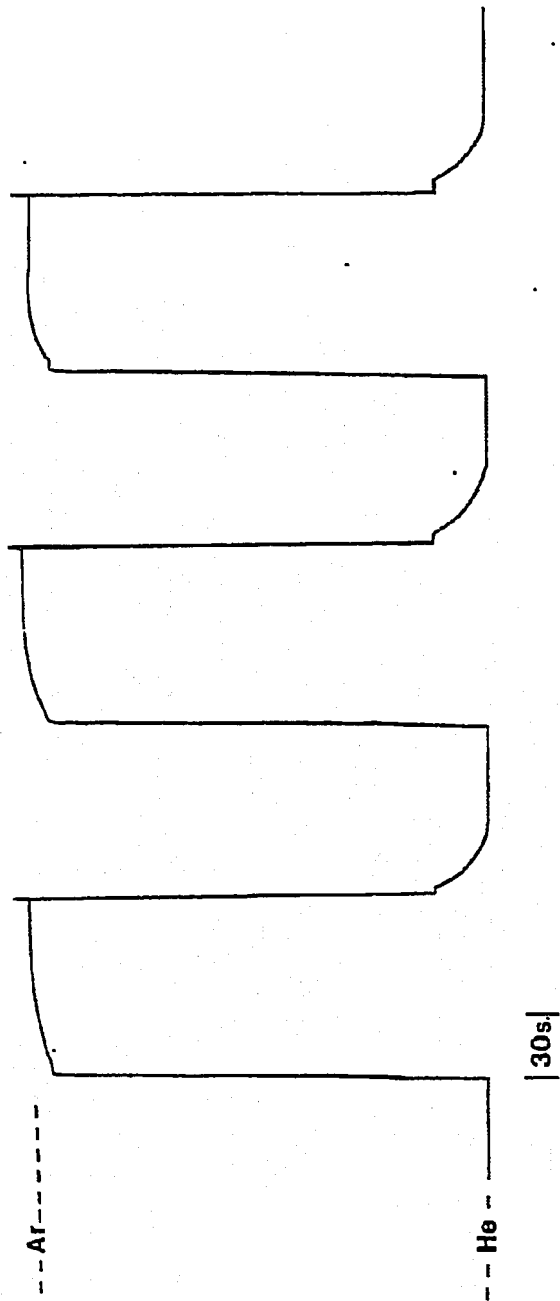
Figure 5.21. The TCD Response for Switching Between Helium and Argon Feeds at 435 Actual mm3/s with 5-Second Feed-Gas Staggering in the Cold-Flow Microreactor Model Using a 20-Micron Distributor Plate. (Experiment 1-3 in Table 5.1).

while the less flexible side was connected to the helium feed-stream
(tap B). The high-pressure side of the transducer was connected to tap
A and to the low-pressure side to tap B.

Typical fast-response differential-pressure traces upon switching
from argon to helium feeding, and from helium to argon feeding are shown
in Figures 5.22 and 5.23, respectively. These traces were taken after
the fourth full cycle. The offset, i.e., positive differential
pressures, indicates that the argon feed-line pressure is slowly
building up over the helium feed-line pressure. This is due to the
greater flexibility of the side of the diaphragm in contact with argon.
These traces also show that the differential pressure between the argon
and helium feed-lines is continuously being adjusted while the plug is
moving. Figure 5.24 is the TCD trace of gas mixing during Experiment
1-9. The striking change produced by the diaphragm installation is the
elimination of the hysteresis effect that was seen in Experiment 1-10
(Figure 5.11) when using the 20-micron distributor in the cold-
flow model.
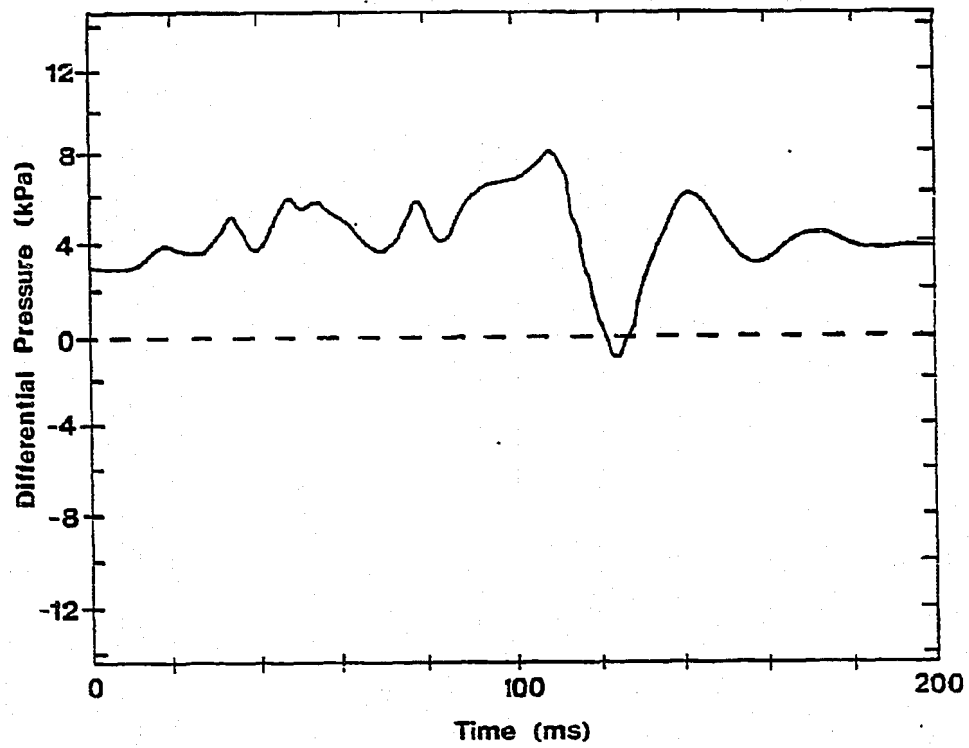
Figure 5.22. The Oscilloscope Trace from a Differential
Pressure Transducer Placed Between the
Helium Feed-Line and the Argon Feed-Line
in Parallel with a Diaphragm. The Argon-
to-Helium Feeding Transitio Is Shown
(Experiment 1-9 in Table 5.1).
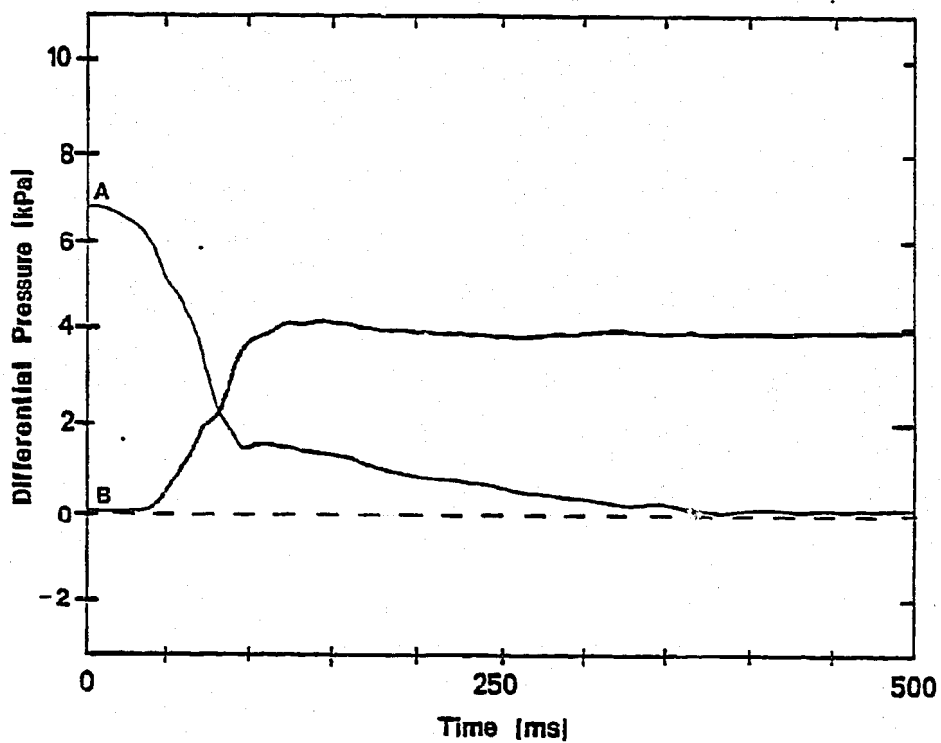
Figure 5.23. The Oscilloscope Trace from a Differential-Pressure Transducer Placed Between the Helium Feed-Line and the Argon Feed-Line in Parallel with a Diaphragm. The Helium-to-Argon Feeding Transition Is Shown. (Experiment 1-9 in Table 5.1).
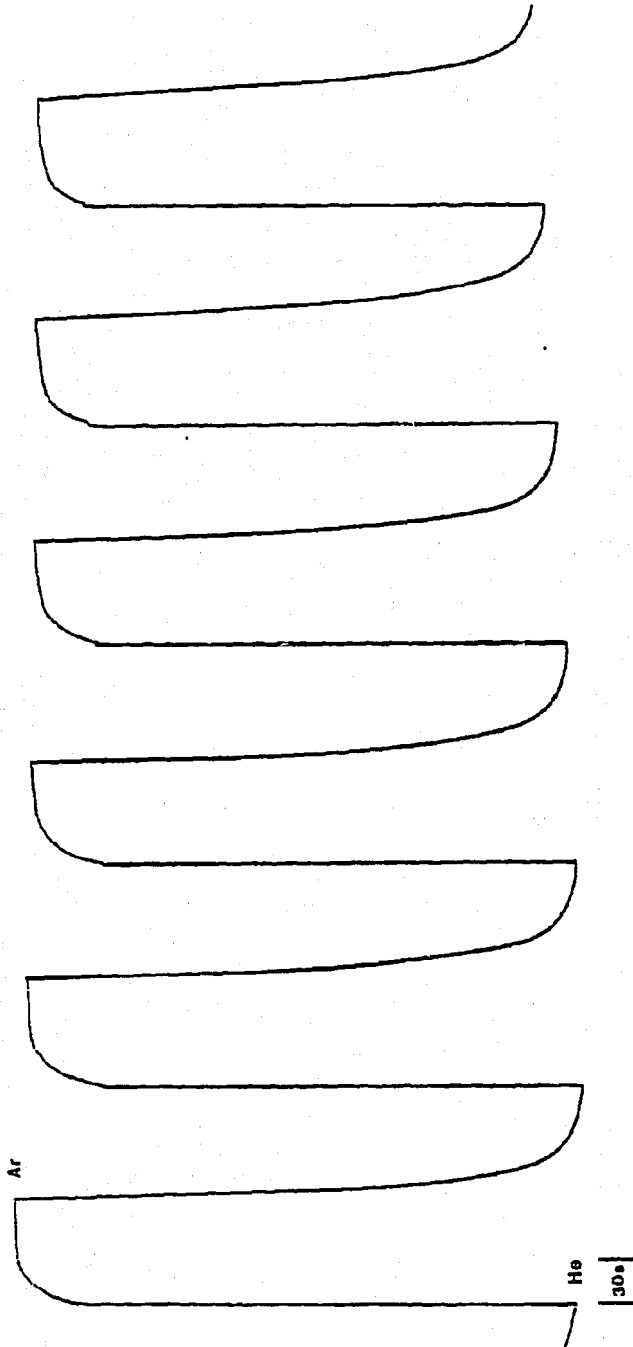
Figure 5.24. The TCD Response for Switching Between Helium and Argon Feeds at
417 Actual mm^3/s with a Diaphragm Between the Feed Lines.
(Experiment 1-9 in Table 5.1).

5.2.3 Cold-Flow Model Experiments Using a 2-Micron Distributor Plate

Experiments in the cold-flow sliding-plug microreactor model using a 20-micron distributor plate pointed to the use of a less porous distributor plate in order to eliminate the gas backflow into the plenum zone. Figure 5.25 is the TCD trace for Experiment 2-2. This experiment is identical to Experiment 1-10 (Figure 5.11) except that a 2-micron distributor plate was used. The flow rate of feed gas was set at 417 actual mm^3/s and the sampling capillary was placed in the plenum zone.

Figure 5.25 shows that a significant improvement has been achieved in both the helium-to-argon and argon-to-helium transitions over those shown in Figure 5.11. The helium-to-argon transition is 97.1% complete in 2.4 seconds after the sliding plug has traversed the plenum, whereas the argon-to-helium transition is 90.2% complete. The hysteresis effect has been eliminated from the helium-to-argon transition and greatly reduced during the argon-to-helium transition. In addition, the final return to the baseline from both transitions has been cut in half to approximately 30 seconds. Fast-response differential-pressure transducer experiments were performed under these conditions with the 2-micron distributor plate in order to check for pressure inversions.

Experiments 2-8 and 2-9 were carried out with the transducer placed between tap A and the catalyst zone, and between tap B and the catalyst zone, respectively. Figures 5.26 and 5.27 show the oscilloscope traces recorded during plug movement for these two experiments. The time-scale differs from that shown in Figures 5.13 and 5.14 in that it has been expanded from 200 ms to 500 ms. The pressure
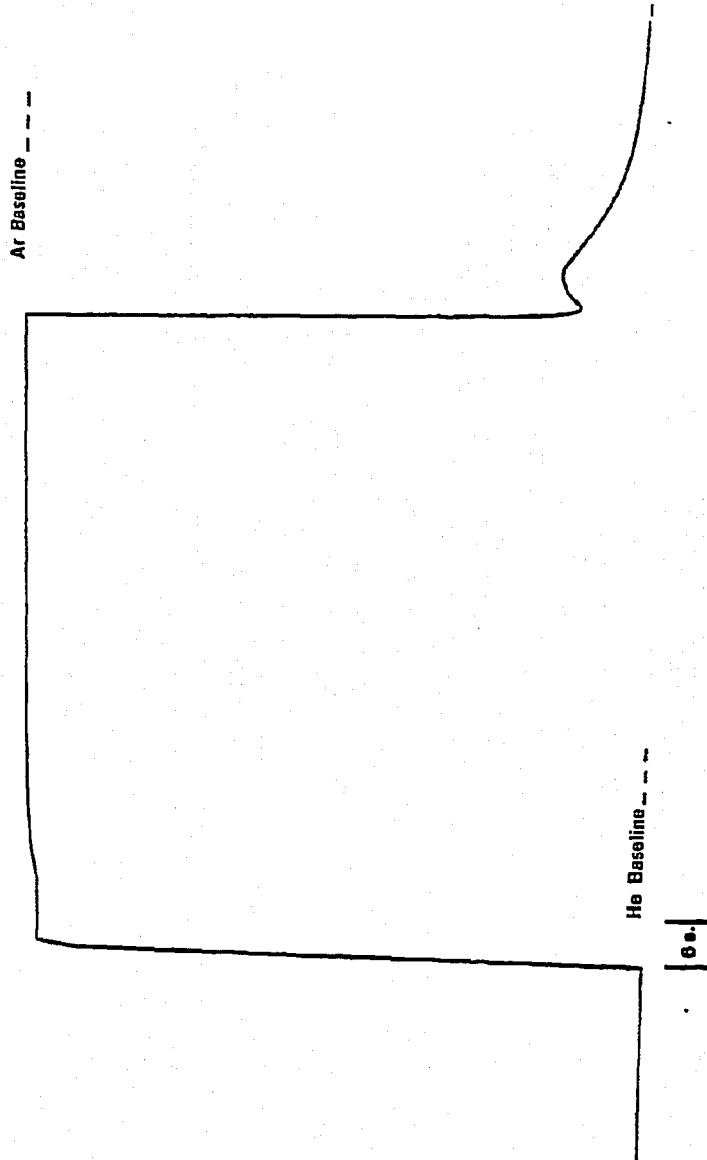
Figure 5.25. The TCD Response for Switching Between Helium and Argon Feeds at
417 Actual mm^3/s in the Cold-Flow Microreactor Model with a 2-
Micron Distributor Plate. (Experiment 2-2 in Table 5.1).
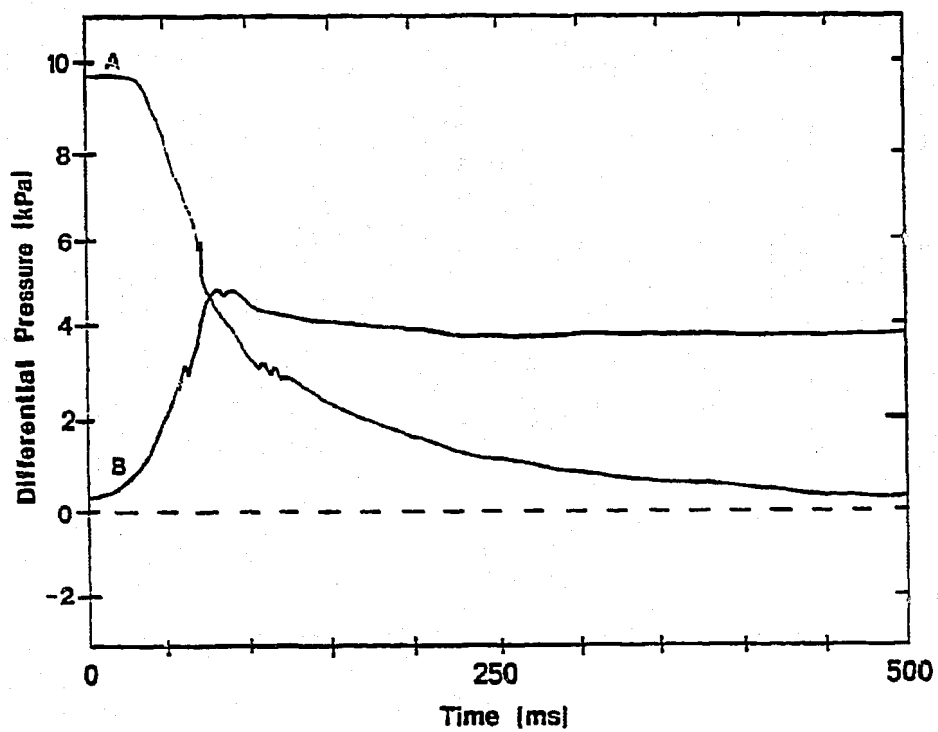
Figure 5.26. An Oscilloscope Trace from a Differential-
Pressure Transducer Placed Between the
Argon Feed-Line (Tap A in Figure 5.1)
and the Catalyst Zone. A 2-Micron Distri-
butor Plate Is in Use. (Experiment 2-8
in Table 5.1). Curve A Is the Helium-
to-Argon Transition and Curve B Is the
Argon-to-Helium Transition.

Figure 5.27. An Oscilloscope Trace from a Differential
Pressure Transducer Placed Between the Helium
Feed-Line (Tap B in Figure 5.1) and the Catalyst
Zone. A 2-Micron Distributor Plate Is in
Use. (Experiment 2-9 in Table 5.1). Curve
A Is the Argon-to-Helium Transition and Curve
B Is the Helium-to-Argon Transition.

inversion has been totally eliminated and the pressure transition after
the plug movement follows a smooth return to the distributor-plate
pressure drop.

After the improvements in reduction of gas mixing utilizing a 2-
micron distributor plate were demonstrated, a series of experiments
were performed in the cold-flow model. This series of experiments had
several goals.

1. To study gas mixing in the plenum zone, catalyst zone, and gas-
exit zone without catalyst vibrofluidization. This was done in order to
determine the influence of the microreactor geometry on gas mixing.

2. To study gas mixing in the catalyst zone and gas-exit zone in
order to determine the extent of gas mixing induced by vibrofluidizing
the catalyst.

3. To study the effect of 5-second staggering on gas mixing in
the plenum zone, catalyst zone, and gas-exit zones both with and without
the catalyst bed being vibrofluidized.

4. To study the effect of feed-gas flow rate on gas mixing during
the experiments involved in items 1 to 3 above. The flow rates used in
these experiments were 417, 833, and 1,650 actual mm^3/sec. Helium and
argon flows were always equal during these experiments. The lowest flow
rate corresponds to the actual flow rate of gas through the microreactor
during the steady-state Fischer-Tropsch studies in the vibrofluidized-
bed microreactor.

The above experiments have been classified as Series 2, 3, and 4
experiments listed in Table 5.1. The results are generally presented

in the form of graphs of the percent transition in 2.4 seconds after the
initial detector response versus feed-gas flow rate. Separate curves
are presented on each plot for the response in the plenum zone, catalyst
zone, and gas-exit zone. A separate graph is offered for the
helium-to-argon and argon-to-helium transitions. A series of bar
graphs interrelate the effects of microreactor geometry, catalyst
vibrofluidization, and feed-gas staggering at a given flow rate. Again,
separate figures are presented for the helium-to-argon and
argon-to-helium transitions. All data presented in graphical form are
contained in Appendix F in the form of thermal conductivity detector
(TCD) output traces.

5.2.3.1 Gas Mixing Induced by Reactor Geometry

Figures 5.28 and 5.29 illustrate the effect of microreactor
geometry on gas mixing when switching from helium to argon, and from
argon to helium at three separate flow rates. The degree of gas mixing
observed in the center of the catalyst zone at 417 actual mm^3/s is
significantly more pronounced than that observed in the plenum. In
addition, upon travelling from the catalyst zone to the gas-exit zone,
considerably more mixing is induced. This trend is more pronounced for
the argon-to-helium transition than for the helium-to-argon transition.
For example, the transition observed in the gas-exit zone at a feed-gas
flow rate of 417 actual mm^3/s is only 42.5% complete after 2.4 seconds
for the argon-to-helium transition. The helium-to-argon transition
shows 78.7% of the transition is complete after 2.4 seconds.

The actual TCD output for this experiment is shown in Figure 5.30.
The difference in the efficiency of gas replacement between helium and
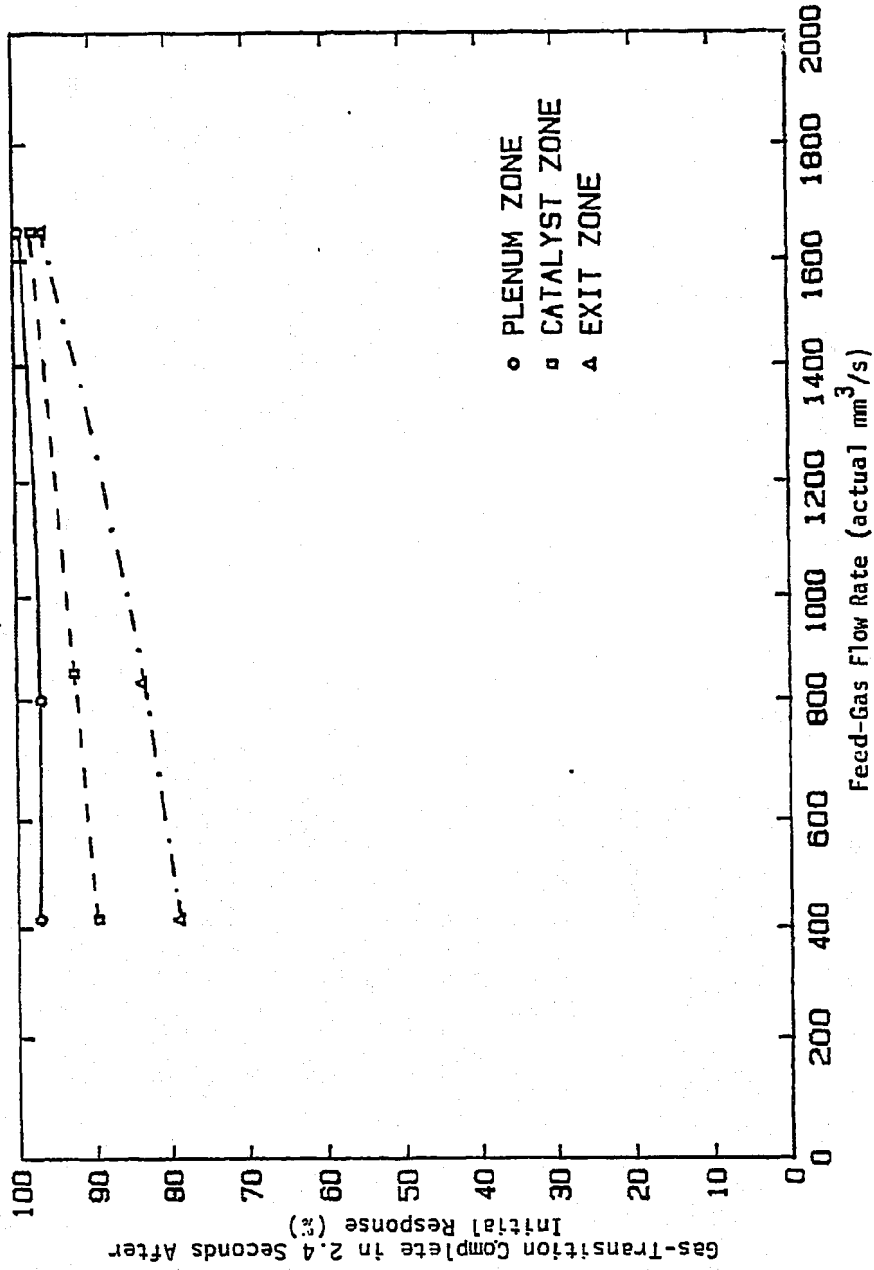
Figure 5.28. The Percent Gas-Transition Complete in 2.4 Seconds After the Initial Detector Responses for the Helium-to-Argon Transition. The Microreactor Model Was Not Vibrated.
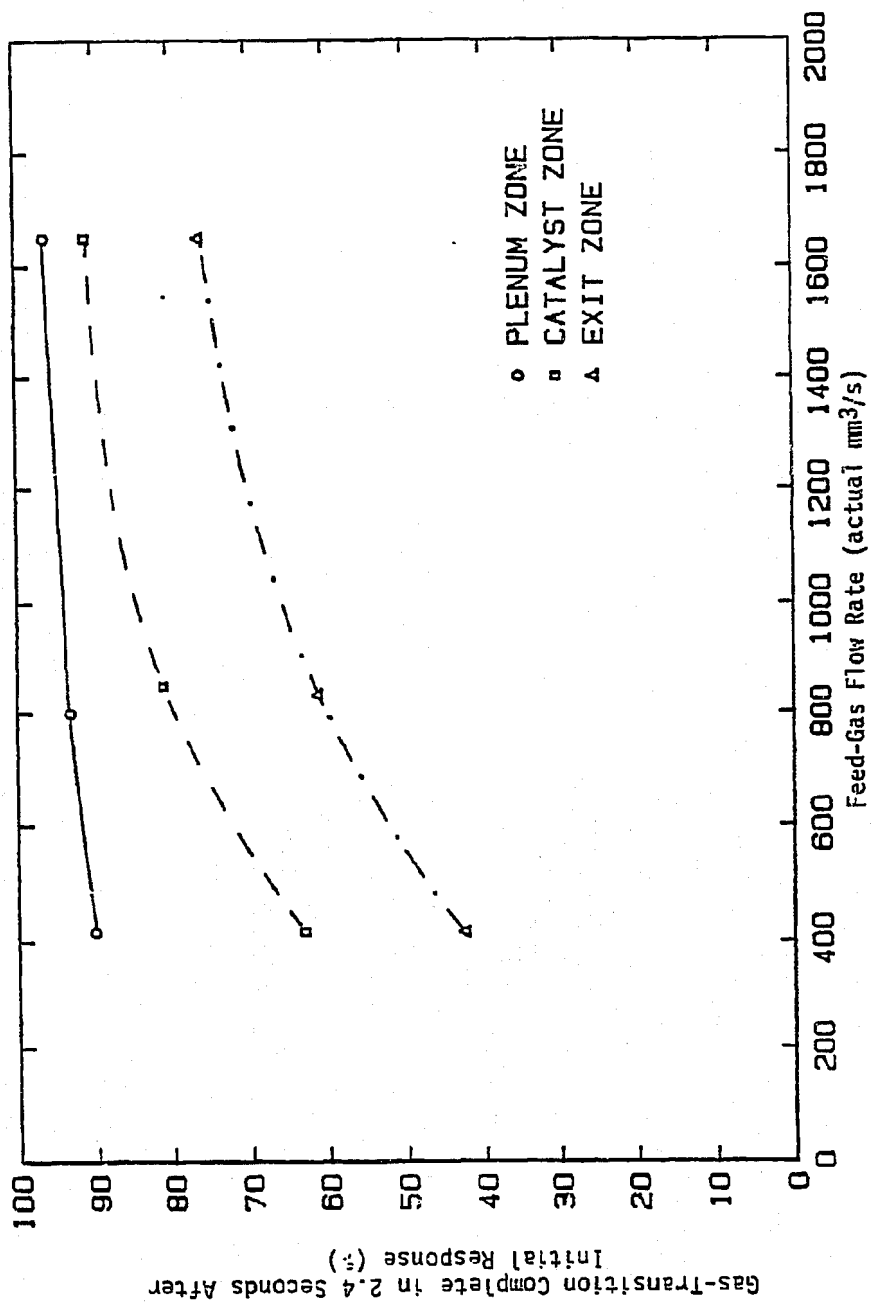
Figure 5.29. The Percent Gas-Transition Complete in 2.4 Seconds After the Initial Detector Responses for the Argon-to-Helium Transition. The Microreactor Model Was Not Vibrated.
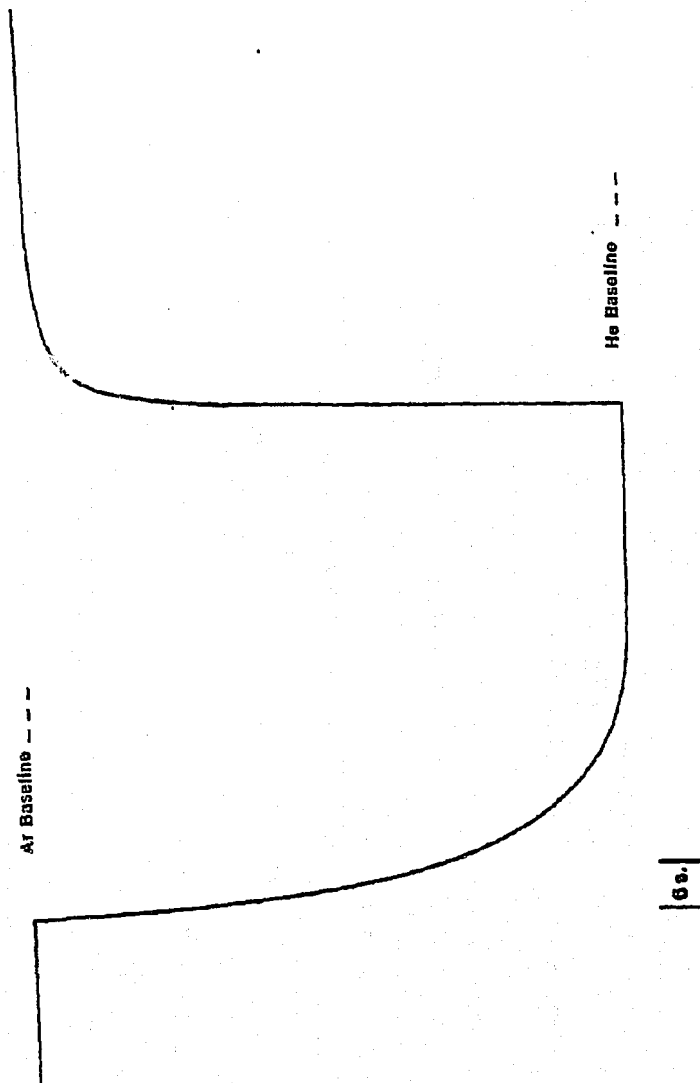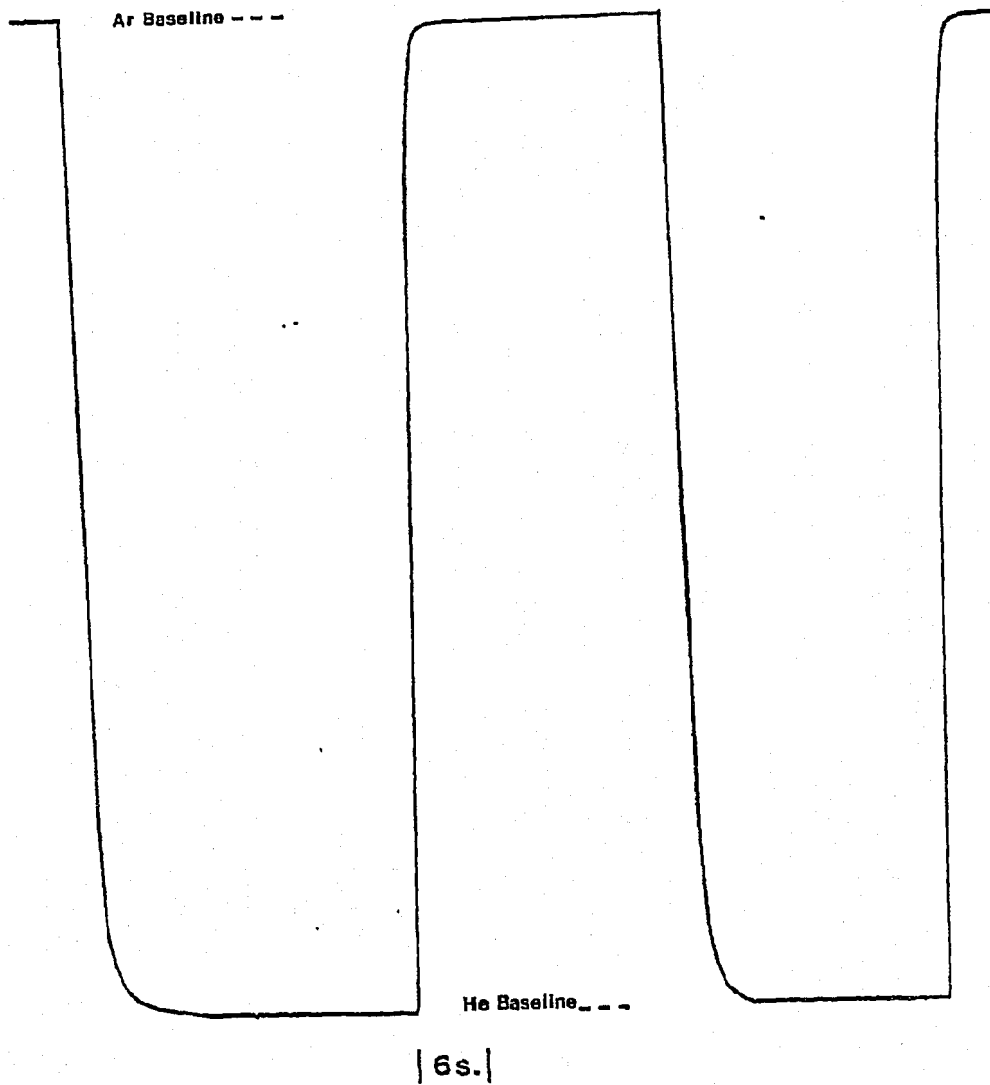
Figure 5.30. The TCD Response for Switching Between Helium and Argon Feeds at 417 Actual mm3/s with Sampling in the Cold-Flow Microreactor Model Exit Zone. (Experiment 4-1 in Table 5.1).

argon is due largely to the difference in their densities. At 25°C and 35 kPa, the density of helium is 0.0727 g/m^3; while argon has a density of 0.726 g/m^3. Therefore, helium is more susceptible to channeling and is not as well-distributed as argon by the distributor plate.

Increasing the flow rate of the feed gases has a significant effect on the degree of gas mixing. The microreactor-induced gas mixing has been greatly reduced. For a feed-gas flow rate of 1650 actual mm^3/s with gas sampling in the plenum zone, the transition is 99.4% complete for the helium-to-argon transition and 96.2% complete for the argon-to-helium transition after 2.4 seconds. The TCD trace under these conditions is shown in Figure 5.31. The transitions produce nearly a square waveform. The helium-to-argon transition is 100% complete within 4 to 5 seconds; while the argon-to-helium transition takes several seconds longer. This suggests that the layer of catalyst directly above the distributor plate is exposed to discrete transitions of feed gas. Again referring to Figures 5.28 and 5.29, similar trends of decreases in gas mixing occur in both the catalyst zone and the gas-exit zone. In the center of the catalyst zone, the transition percent after 2.4 seconds has been increased to 97.0% and 91.0% for the helium-to-argon and argon-to-helium switches, respectively at a feed gas flow rate of 1650 actual mm^3/s .

5.2.3.2 Gas Mixing Induced by Catalyst Vibrofluidization

As stated in Section 2.4, one characteristic long attributed to vibrofluidized beds is the lack of gas backmixing under certain conditions. The effect of vibrofluidizing 1 gram of -150+300 u fused-

Figure 5.31. The TCD Response for Switching Between Helium and Argon Feeds at 1650 Actual mm^3/s with Sampling in the Cold-Flow Microreactor-Model Plenum Zone. (Experiment 2-12 in Table 5.1).

iron catalyst in the catalyst zone of the cold-flow microreactor model was studied. It was found that vibrofluidization in the catalyst zone did not affect the gas mixing in the plenum zone. There was, however, a change in the degree of gas mixing as measured in the center of the catalyst zone and in the gas-exit zone.

Figure 5.32 illustrates the influence of feed-gas flow rate on the helium-to-argon transition during vibrofluidization. When comparing Figure 5.32 to Figure 5.28 (with no vibrofluidization), several differences are apparent. The degree of gas mixing in the catalyst zone has increased, shifting that curve down an average of 5% from Figure 5.28 to 5.32. At the lower gas flow rates, the degree of mixing measured at the sampling point in the gas-exit zone did not change significantly with the introduction of vibration. However, at a flow rate of 1650 actual mm^3/s, the transition percentage dropped 5 points. This indicates that the replacement of helium by argon, to a noticeable degree, is influenced by the virbofluidized catalyst in the catalyst zone. At low flow rates, most of the increase in mixing is induced below the center of the catalyst section, where the sampling point is located. However, at a flow of 1650 actual mm^3/s, a significant extent of the mixing induced by vibrofluidization occurs above the center of the catalyat zone.

The effect of vibrofluidization on the argon-to-helium transition at several flow rates is illustrated in Figure 5.33. Comparing this plot to Figure 5.29 where no vibrofluidization was induced brings out several difference. The introduction of vibrofluidization has again
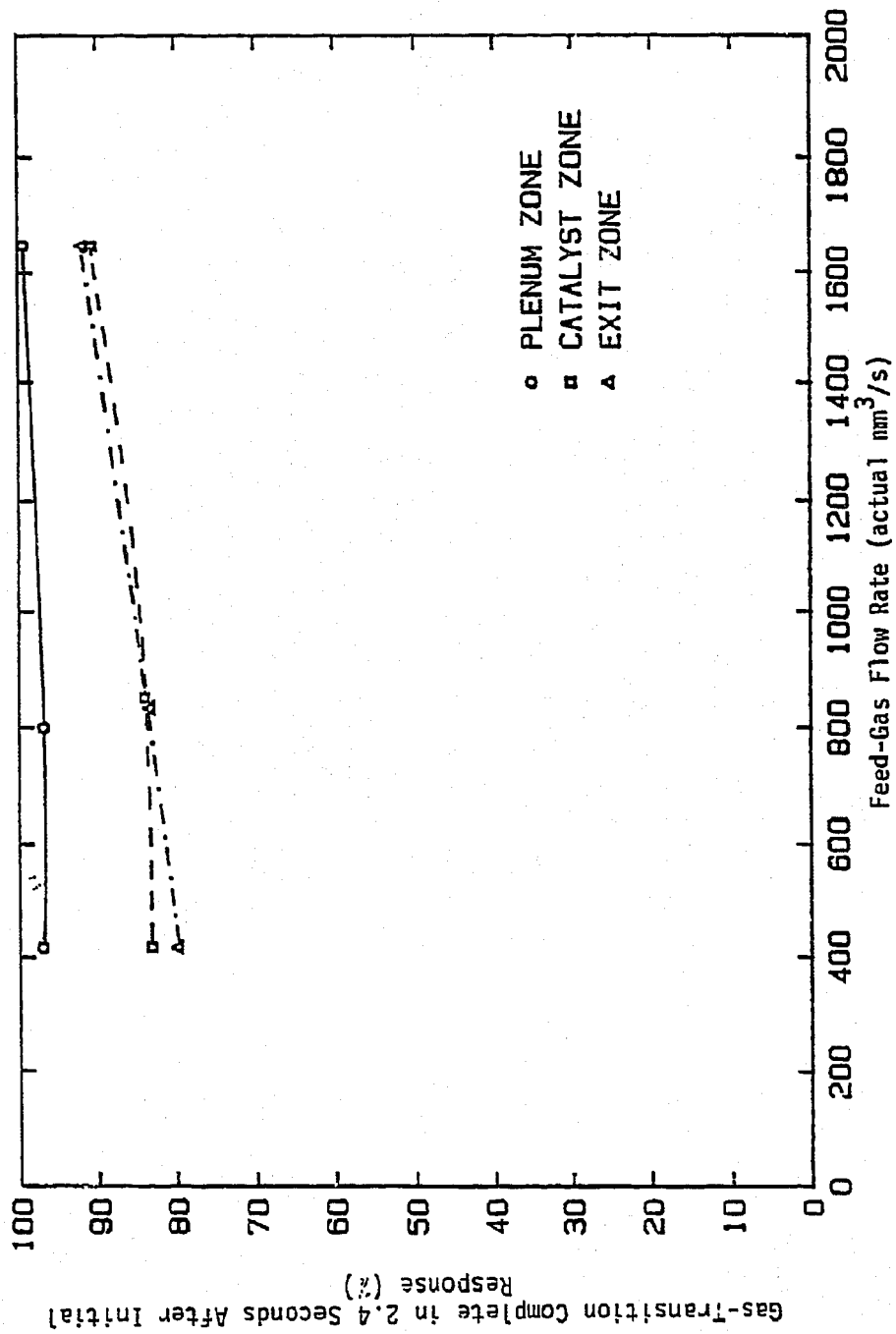
Figure 5.32.   The Percent Gas-Transition Complete in 2.4 Seconds After the Initial Dectector Responses for the Helium-to-Argon Transition. The Microreactor Model Was Vibrated.
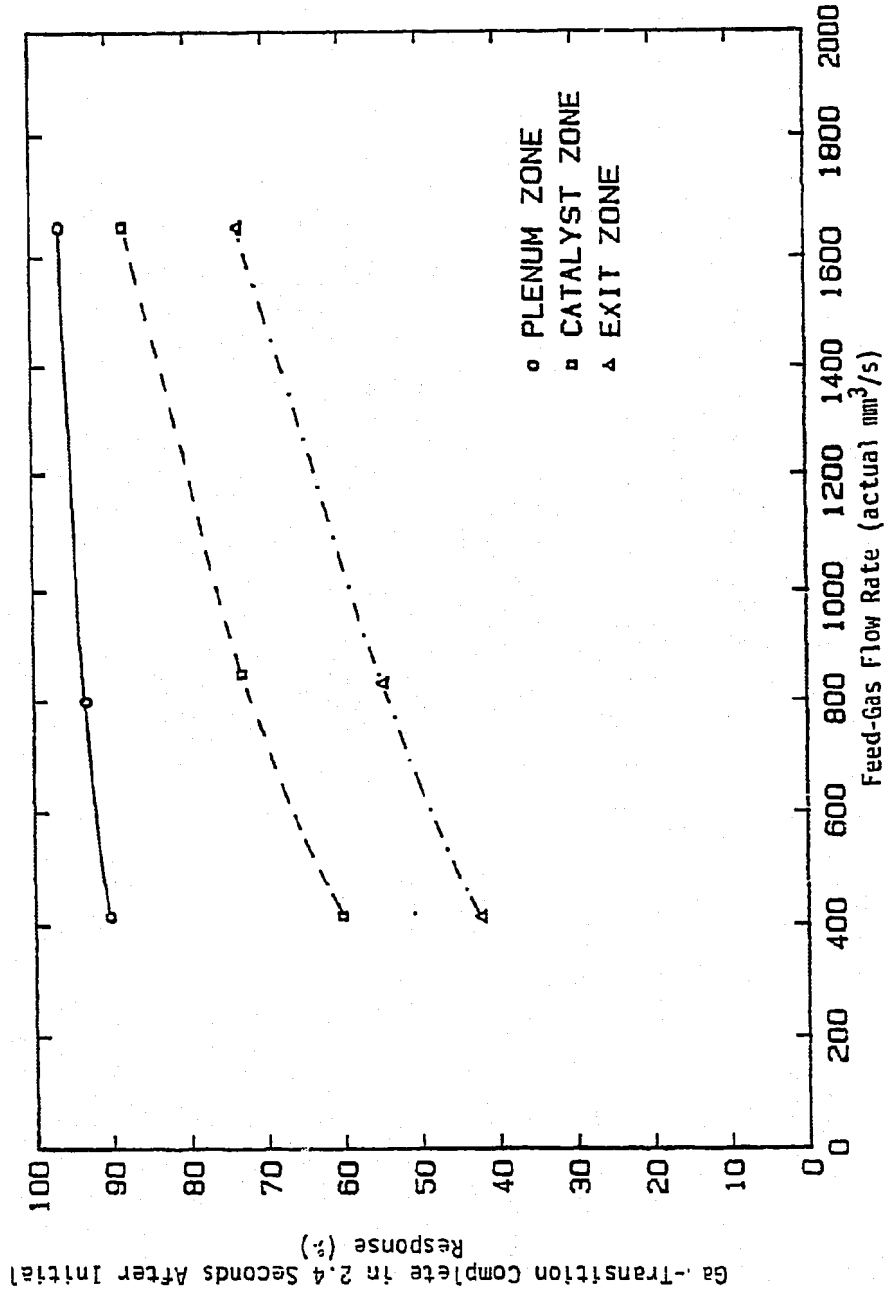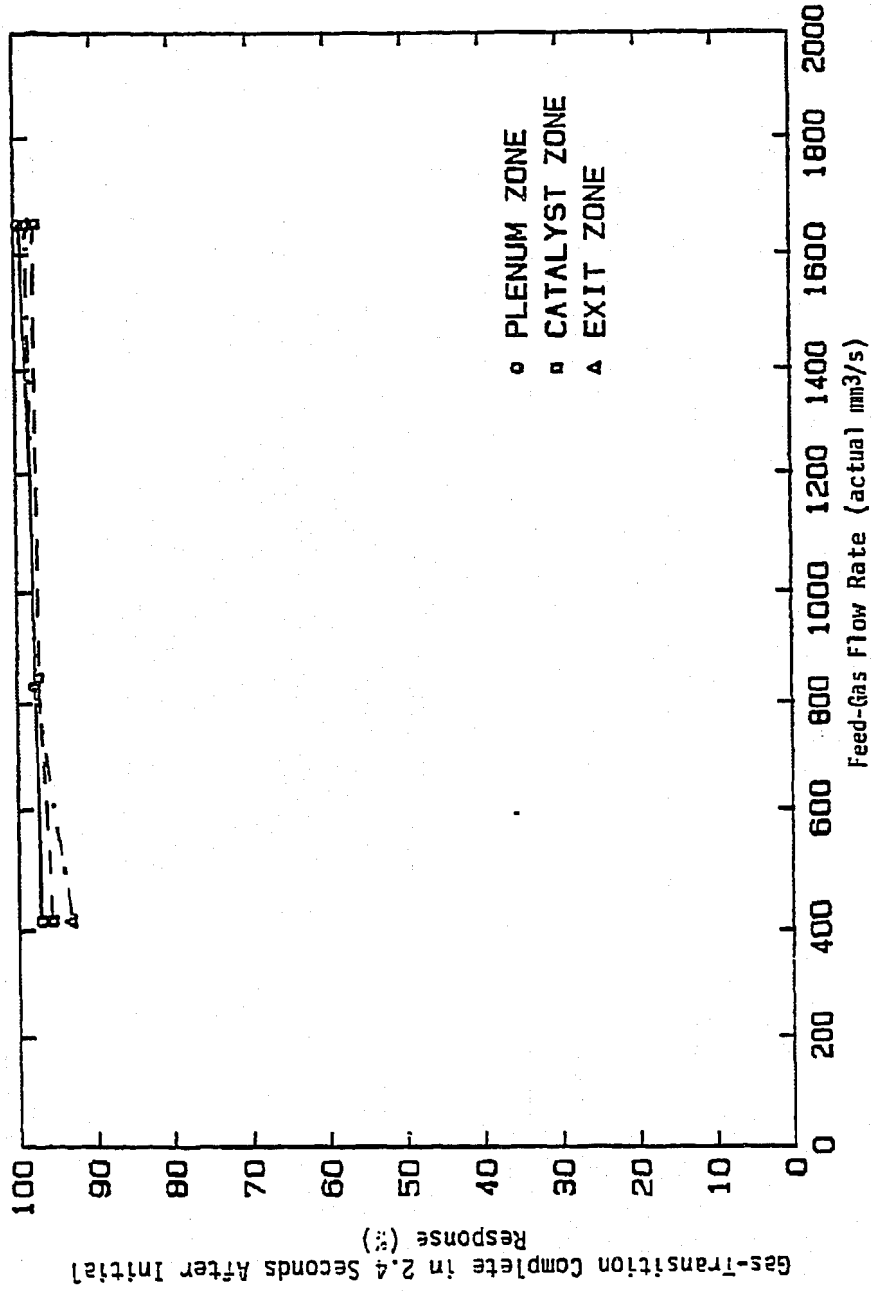
Figure 5.33. The Percent Gas-Transition Complete in 2.4 Seconds After the Initial Dectector Responses for the Argon-to-Helium Transition. The Microreactor Model Was Vibrated.

reduced the percentage of the argon-to-helium transition in the catalyst zone and gas-exit zone. The effect is minimal at 417 and 1650 actual mm^3/s and more pronounced at 833 actual mm^3/s. At a flow rate of 833 actual mm^3/s, the percent transition has dropped from 81.1 to 73.0% at the center of the catalyst zone. Similarly, it dropped from 61.0 to 54.7% at the sampling point in the gas-exit zone.

5.2.3.3 Effect of Staggering on Gas Mixing

Figures 5.34 and 5.35 illustrate the effect of 5-second staggering on the helium-to-argon and argon-to-helium transitions as a function of feed-gas flow rate. The catalyst bed is not being vibrated in the results shown here. Five-second staggering produces an initial burst of gas through the catalyst zone, immediately after the plug has traversed the plenum. For a feed-gas flow rate of 417 actual mm^3/s, the volume of gas going through the catalyst zone during this burst is approximately 2,085 mm^3. Since the volume of the catalyst zone is 1,152 mm^3, the gas in the zone is replaced 1.8 times by this initial burst. For a 5-second staggering with a flow rate of 833 actual mm^3/s, the gas in the catalyst zone is replaced 3.6 times by the initial burst.

At a flow rate of 1,650 actual mm^3/s, the 5-second staggering turns the gas in the catalyst zone over approximately 7.2 times immediately after plug movement. The result of this rapid burst of gas is illustrated in Figure 5.34 for the helium-to-argon transition. The percent transition after 2.4 seconds is greater than 90% in all cases.

Figure 5.35 shows the staggering results for the more difficult argon-to-helium transition. Note that the argon-to-helium transition

Figure 5.34.   The Percent Gas-Transition Complete in 2.4 Seconds After the Initial Dectector
Responses for the Helium-to-Argon Transition. Five-Second Feed-Gas
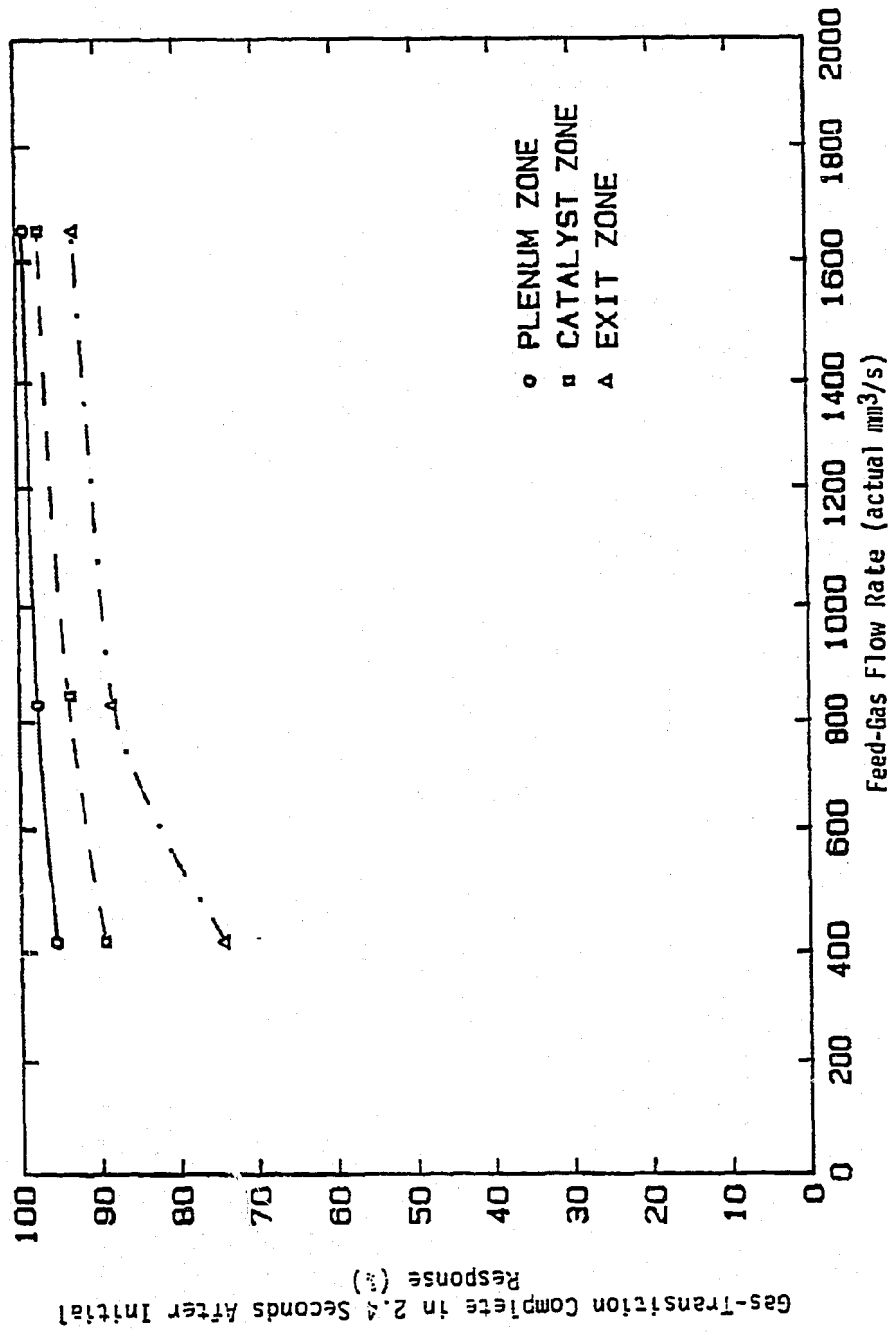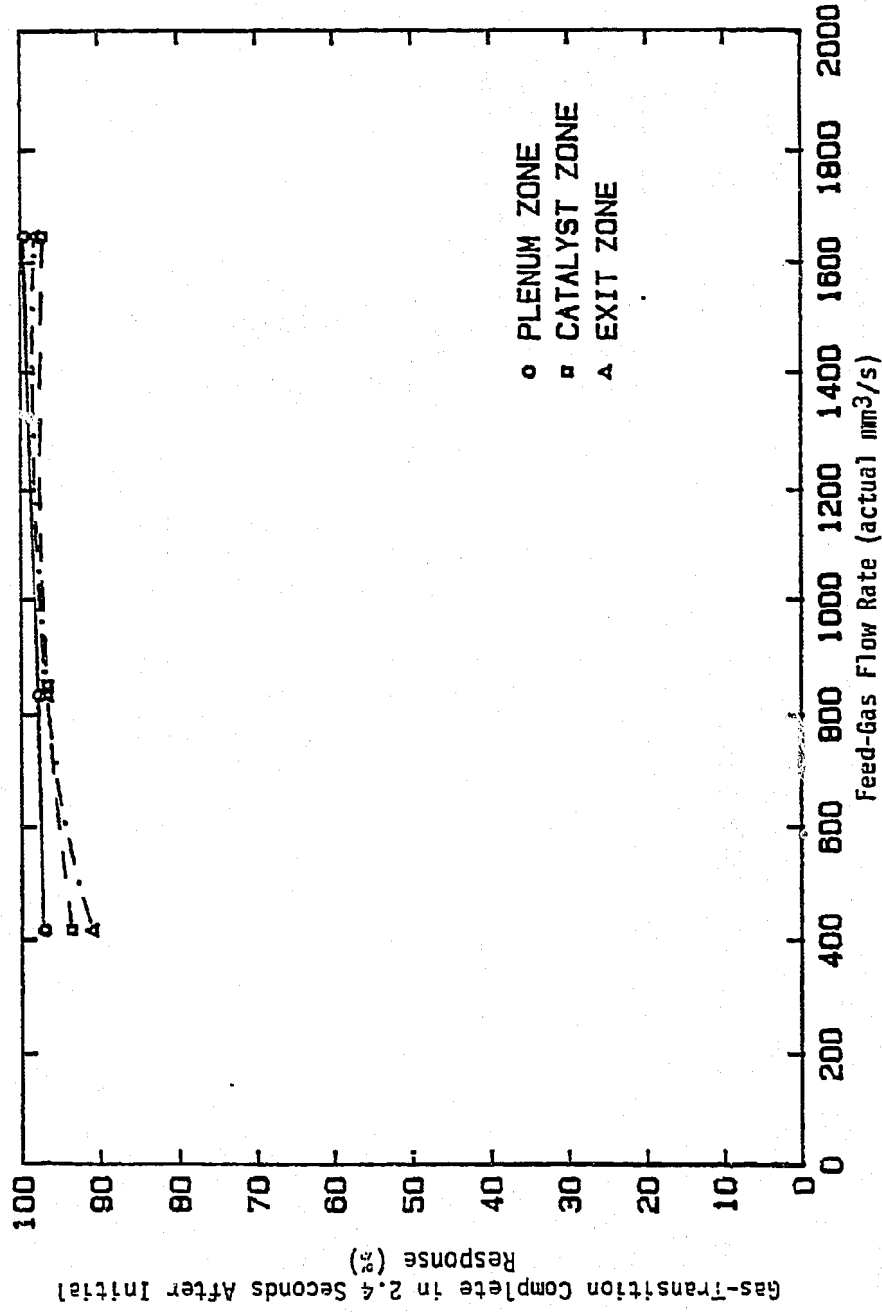Staggering Was Used.

Figure 5.35. The Percent Gas-Transition Complete in 2.4 Seconds After the Initial Dectector Responses for the Argon-to-Helium Transition. Five-Second Feed-Gas Staggering Was Used.

is difficult because helium is much less dense than argon. Again, in the plenum and catalyst zones, the transitions are greater than 90% complete after 2.4 seconds for all flow rates. In addition, the gas mixing observed at the gas-exit sampling point has been decreased when compared to the case with no staggering (Figure 5.29). With no staggering at 417 actual mm^3/s, the transition was only 42.5 percent complete in this period. At the same flow rate the transition had improved to 74.1 percent using 5-second staggering.

Figures 5.36 and 5.37 display the results of introducing 5-second feed-gas staggering, while the catalyst bed is vibrofluidized. The results for the helium-to-argon transition with (Figure 5.36) and without (Figure 5.34) vibrofluidization are nearly identical. The only significant difference is for feed-gas flow rates of 417 actual mm^3/s, where the resulting transition with vibrofluidization is 2 to 3% slower in the catalyst and gas-exit zones. For the argon-to-helium transition, the extent of gas mixing with 5-second staggering is significantly greater when the catalyst bed is vibrofluidized.

An examination of Figure 5.37 in comparison with Figure 5.35 shows that the introduction of the vibrofluidized catalyst bed causes a 12% decrease in gas-transition completion at 417 actual mm^3/s in the catalyst zone. Overall at this flow rate, the sample taken from the gas-exit zone shows a new 7-percent decrease in gas-transition completion. As flow rate is increased, the backmixing effect of vibrofluidization on the feed gases decreases, finally resulting in nearly identical, rapid transitions at 1,650 actual mm^3/s.

238

Figure 5.36. The Percent Gas-Transition Complete in 2.4 Seconds After the Initial Dectector Responses for the Helium-to-Argon Transition. Five-Second Feed-Gas Staggering and Vibrofluidization Were Used.
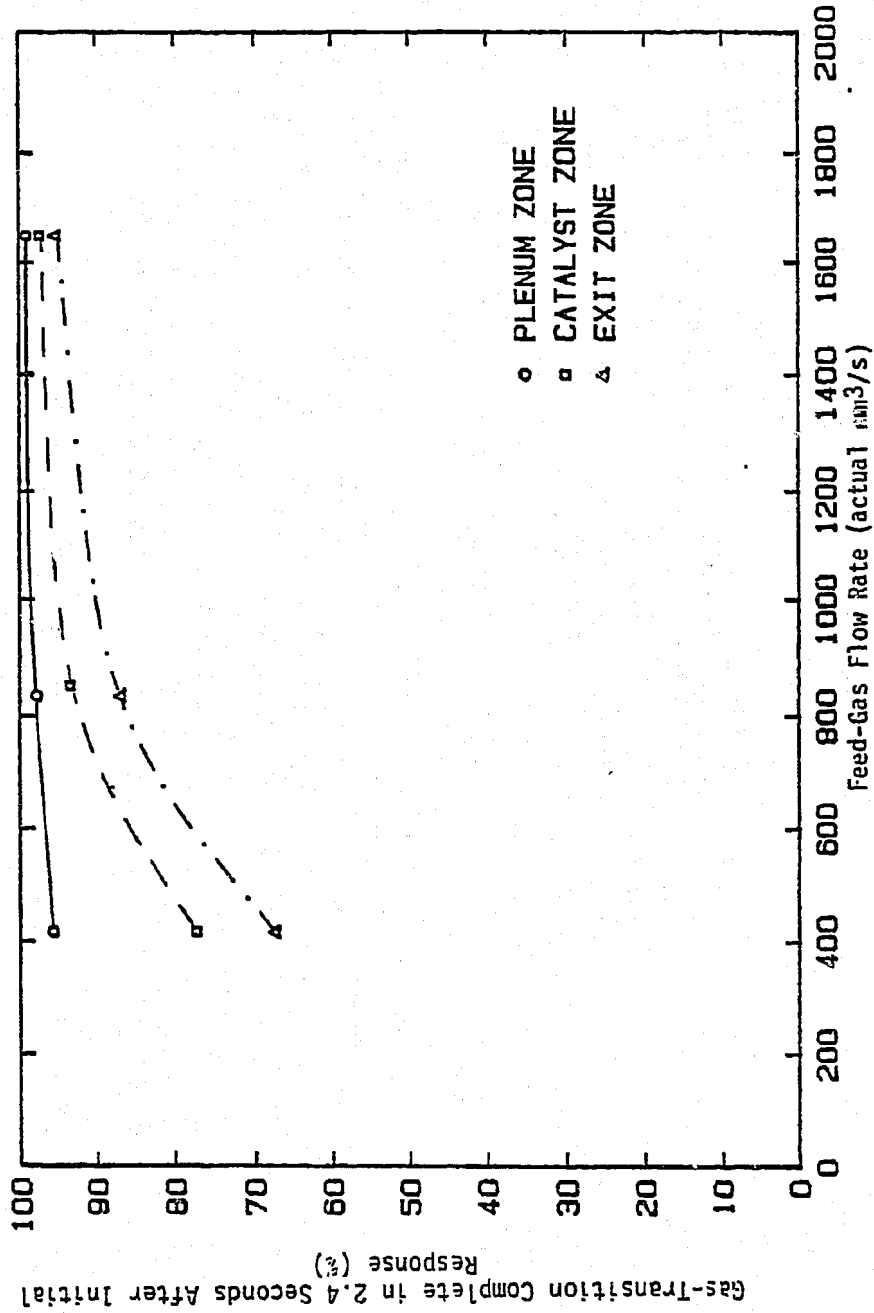
Figure 5.37. The Percent Gas-Transition Complete in 2.4 Seconds After the Initial Dectector Responses for the Argon-to-Helium Transition. Five-Second Feed-Gas Staggering and Vibrofluidization Were Used.

5.2.3.4 Trends in Gas Mixing

Figures 5.38-5.43 summarize the trends in gas mixing in the cold-flow microreactor model. Each bar graph presents the percent of gas-transition completion as a function of the sampling point in the microreactor, 2.4 seconds after the initial detector response. The sampling points were placed in the plenum zone, the catalyst zone and the gas-exit zone. Two bars are presented for the plenum zone representing results from experiments with and without feed-gas staggering. Note that vibrofluidation in the catalyst zone has not been found to affect gas mixing in the plenum zone. Four bars are presented for both the catalyst zone and the gas-exit zone.

The bars in Figures 5.39-5.43 represent the following:

bar 1: percent transition during catalyst vibrofluidization

bar 2: percent transition without catalyst vibrofluidization

bar 3: percent transition with 5-second staggering but without vibrofluidization

bar 4: percent transition with both 5-second staggering, and vibrofluidization

A separate figure is presented for the helium-to-argon and argon-to-helium transitions at each of the three feed-gas flow rates studied.

As can be seen from these graphs, the introduction of catalyst vibrofluidization causes an increase in gas mixing, resulting in the decrease in percent gas-transition completion represented. Most of the backmixing caused by vibrofluidization of the catalyst is experienced in the lower half of the catalyst zone, below the sampling point.
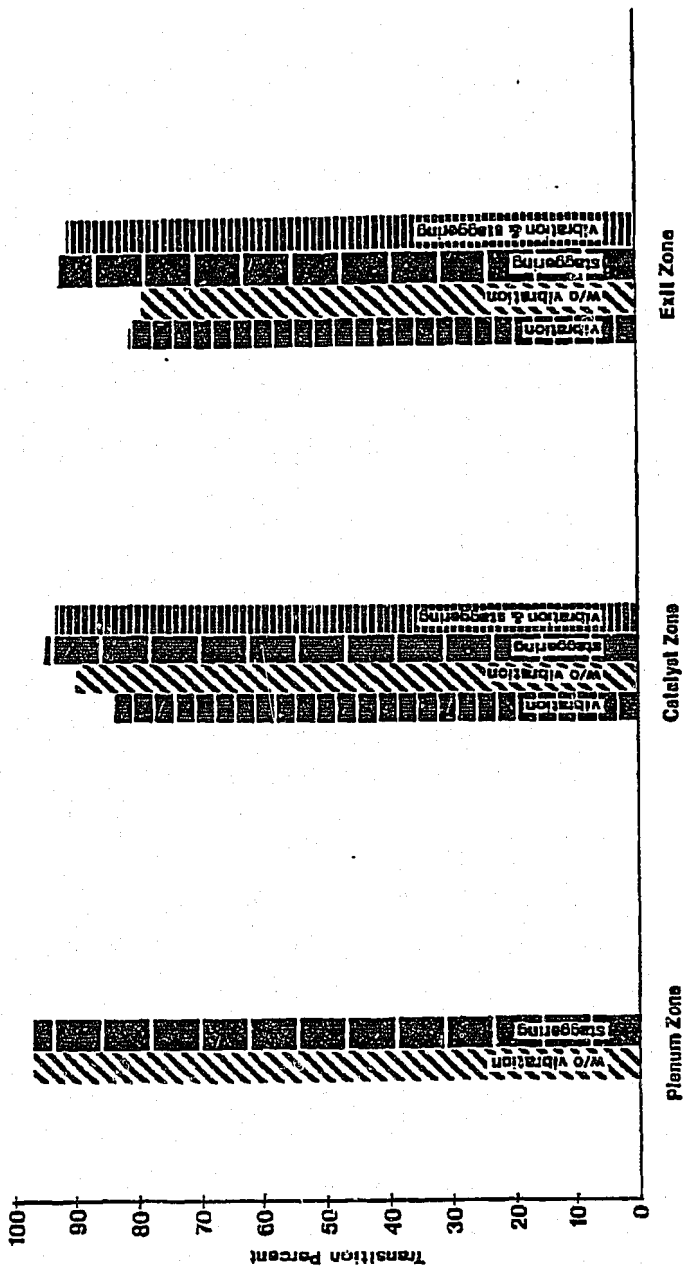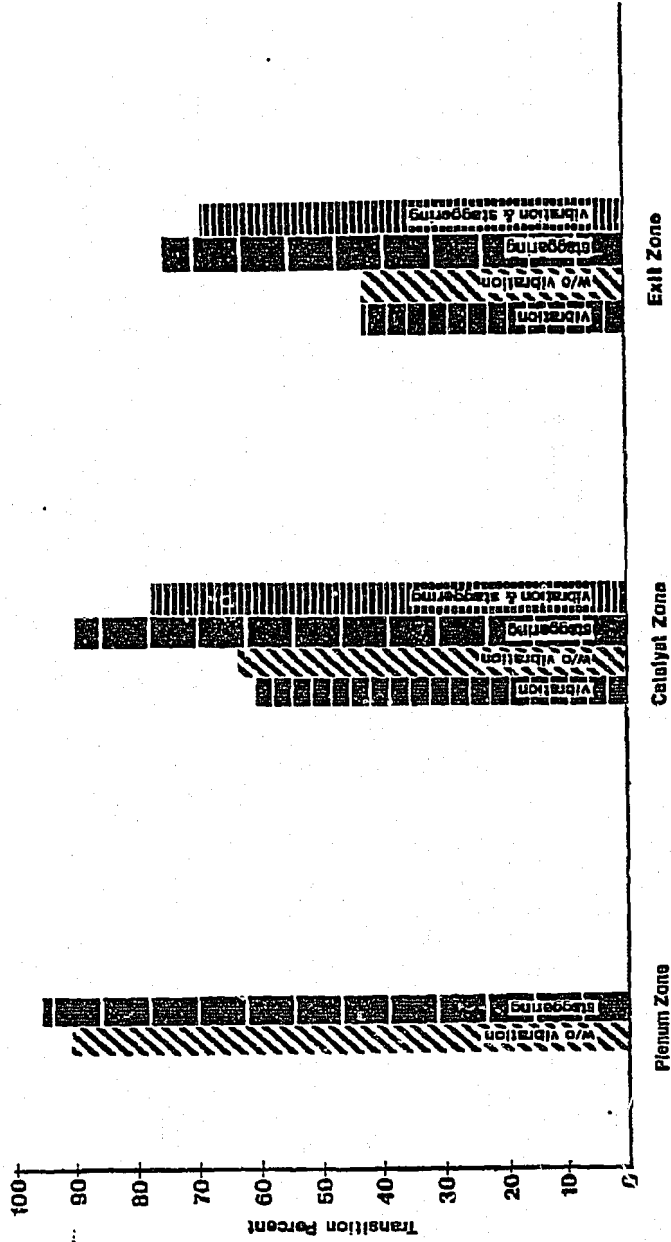
Figure 5.38. A Summary of Percent Gas-Transition Completion in the Cold-Flow Micro-reactor 2.4 Seconds After the Initial Detector Response. Shown Is the Helium-to-Argon Feed Transition at 417 Actual mm3/s.

Figure 5.39. A Summary of Percent Gas-Transition Completion in the Cold-Flow Micro-
reactor 2.4 Seconds After the Initial Detector Response. Shown Is the
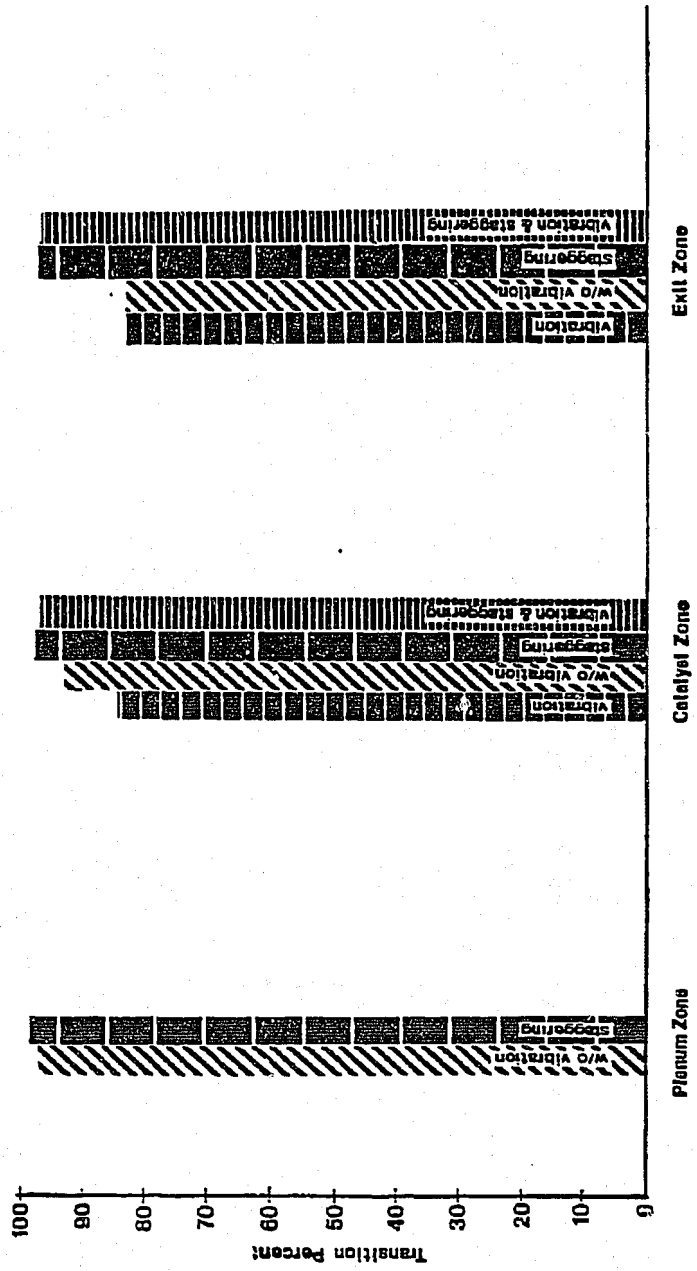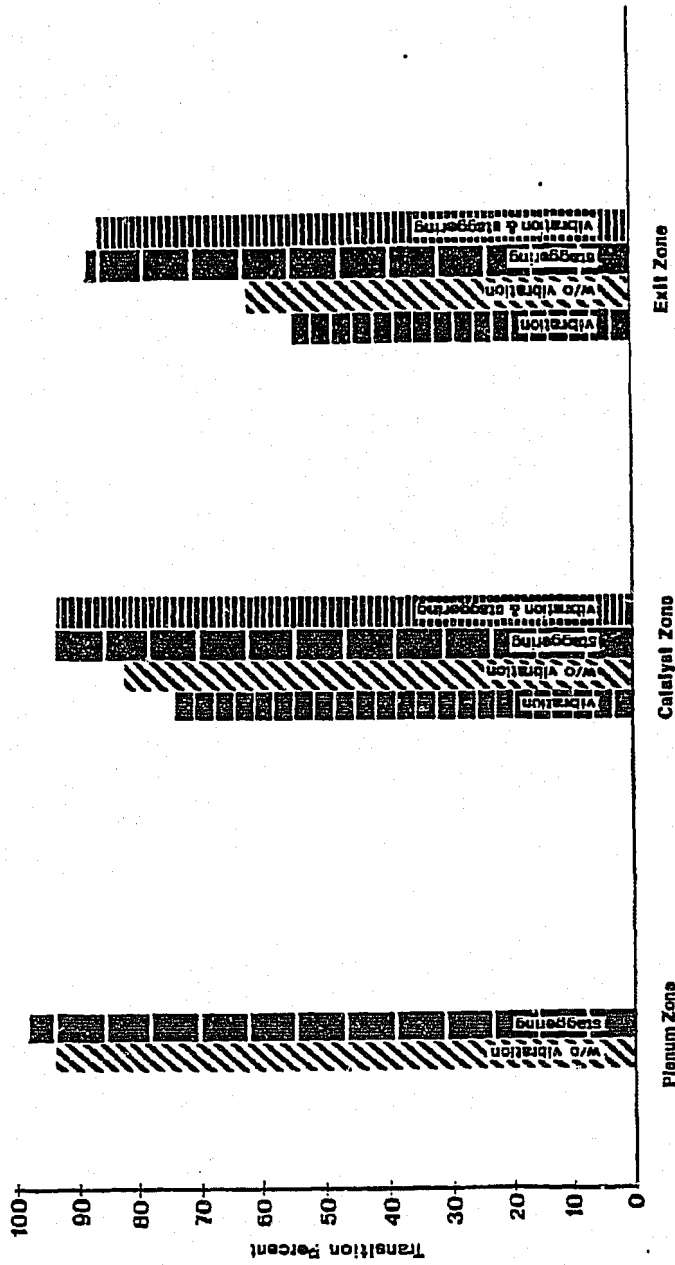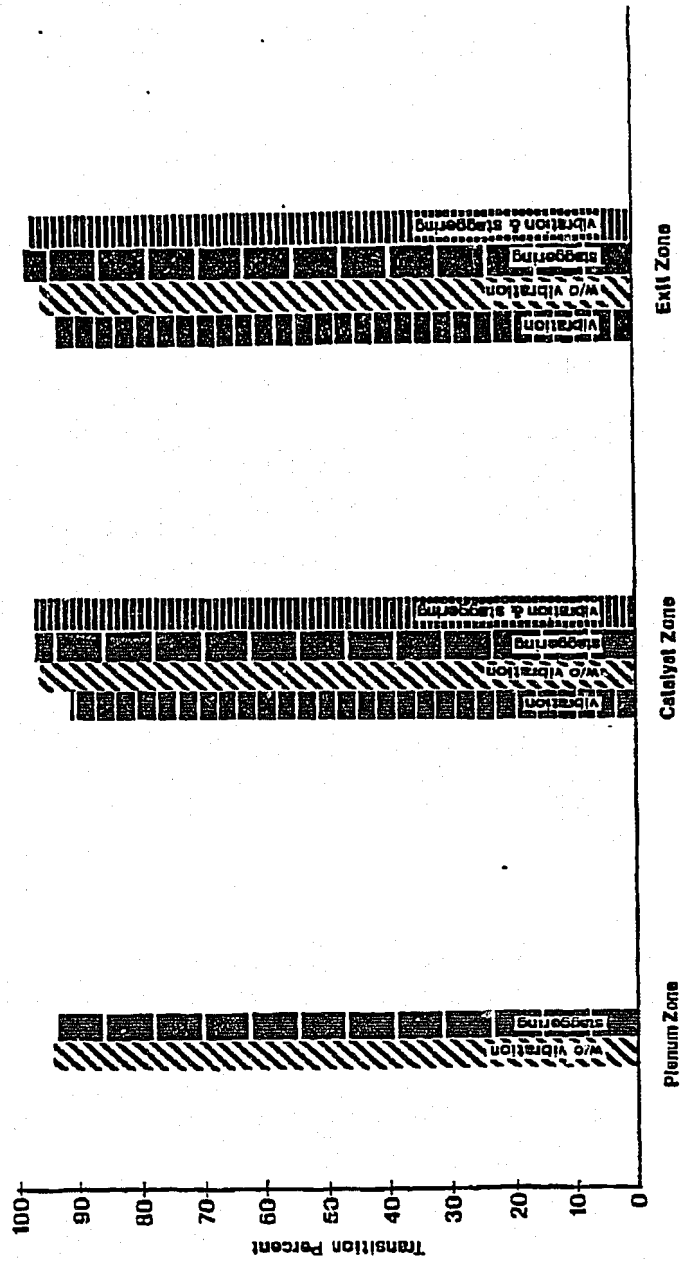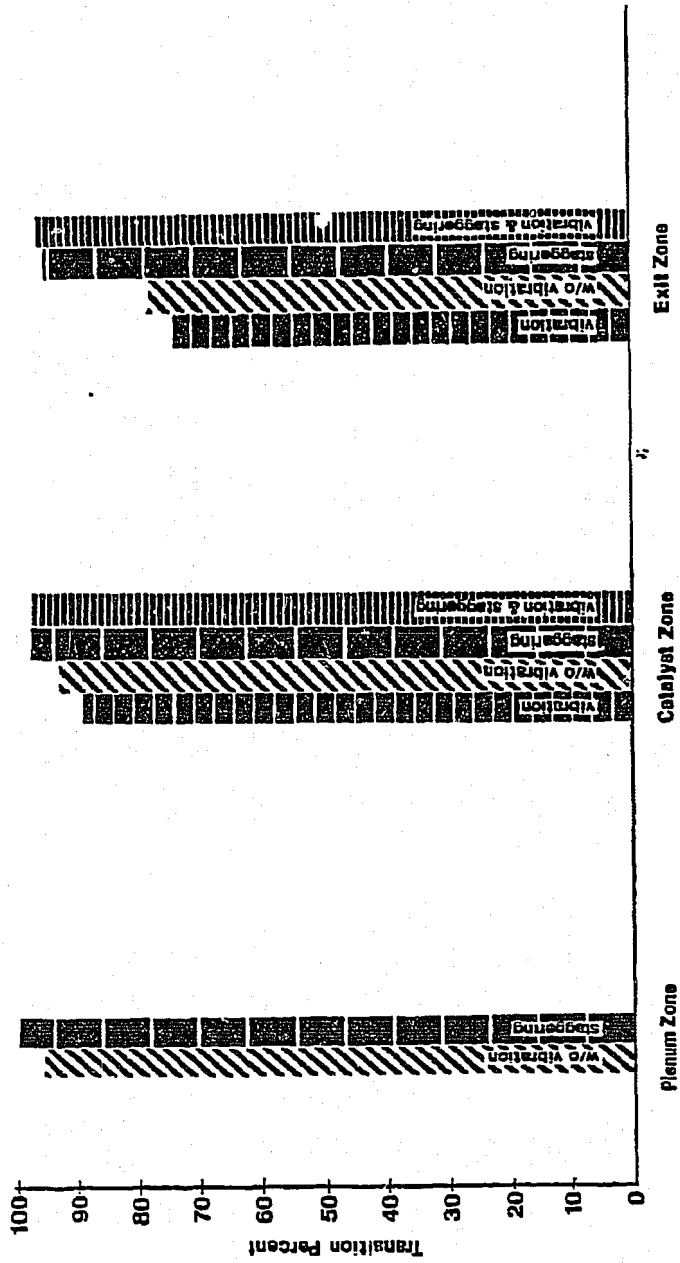Argon-to-Helium Feed Transition at 417 Actual mm3/s.

Figure 5.40. A Summary of Percent Gas-Transition Completion in the Cold-Flow Micro-reactor 2.4 Seconds After the Initial Detector Response. Shown Is the Helium-to-Argon Feed Transition at 833 Actual mm^3/s.

244

Figure 5.41. A Summary of Percent Gas-Transition Completion in the Cold-Flow Micro-reactor 2.4 Seconds After the Initial Detector Response. Shown Is the Argon-to-Helium Feed Transition at 833 Actual nm^3/s.

Figure 5.42. A Summary of Percent Gas-Transition Completion in the Cold-Flow Micro-reactor 2.4 Seconds After the Initial Detector Response. Shown Is the Helium-to-Argon Feed Transition at 1650 Actual mm3/s.

Figure 5.43. A Summary of Percent Gas-Transition Completion in the Cold-Flow Micro-reactor 2.4 Seconds After the Initial Detector Response. Shown Is the Argon-to-Helium Feed Transition at 1650 Actual mm^3/s.

Staggering of the feed gas results in a significant reduction in gas mixing as expressed in the increase in percent gas-transition completion. This is the case when the catalyst is vibrofluidized and when it is not. Staggering produces a greater percentage improvement for the argon-to-helium transition than for the helium-to-argon transition. Also, the improvement is greater at the lower feed-gas flow rate. In general, the helium-to-argon transition is much more rapid than the argon-to-helium transition, presumably due to the density difference of the gases. When compared to argon, helium is more likely to channel through the distributor plate, the catalyst bed and the catalyst retention plate. Argon, however, is more apt to push out the less dense helium and is not as prone to bypassing.

The main objectives of this cold-flow model study were to identify conditions which produce discrete pulses of helium and argon below the catalyst bed, and to determine the gas-mixing properties of the vibrofluidized bed. Notable reductions in gas-mixing have been achieved, as expected, through the use of higher gas flow rates and feed-gas staggering.

The limitation of using high gas flow rates is that under F-T synthesis conditions, an increase in flow rate at constant pressure will cause a parallel increase in space velocity. An effective means to avoid using high gas flow rates would be to decrease the system pressure. The space velocity, and therefore the conversion, could be maintained constant and the transition to a new gas upon sliding-plug movement would be more discrete.

Feed-gas staggering causes a sudden burst of gas through the reaction zone of the microreactor followed by a much lower, constant gas flow rate. The space velocity through the reactor would consequently follow the same pattern. If equal gas flow rates are used, a uniform space velocity through the catalyst bed results.

5.2.4 Characteristics of the Vibrofluidized Bed of Catalyst

This study is the first to use a shallow vibrofluidized bed of catalyst to simulate the solids mixing characteristics of a gas-fluidized bed. As stated earlier, one gram of -150+300 μ fused-iron catalyst is used in the reaction zone (3.18-mm wide, 25.4-mm long and 14.29-mm deep) of the microreactor. In reference to the cold-flow model, this zone has been called the catalyst zone. The catalyst is vibrofluidized by imparting a vertical motion to the microreactor using a vibrator and an associated support structure. The microreactor is vibrated at the resonance frequency of the leaf-spring support system, typically 18 to 25 Hz. The peak-to-peak amplitude of vibration, as measured at the microreactor, is approximately 4 mm. The static bed height of the catalyst in the reaction zone is approximately 4.3 mm, thus occupying nearly one-third of the volume.

Figure 5.44 is a photograph of the catalyst zone of the cold-flow microreactor model, showing the static bed height. The sliding plug has been captured in mid-motion as it traverses the plenum zone.

Figure 5.45 shows two photographs of the catalyst bed as it is being vibrofluidized at a frequency of 24 Hz and a peak-to-peak amplitude of 4 mm. These photographs are typical of the bed behavior
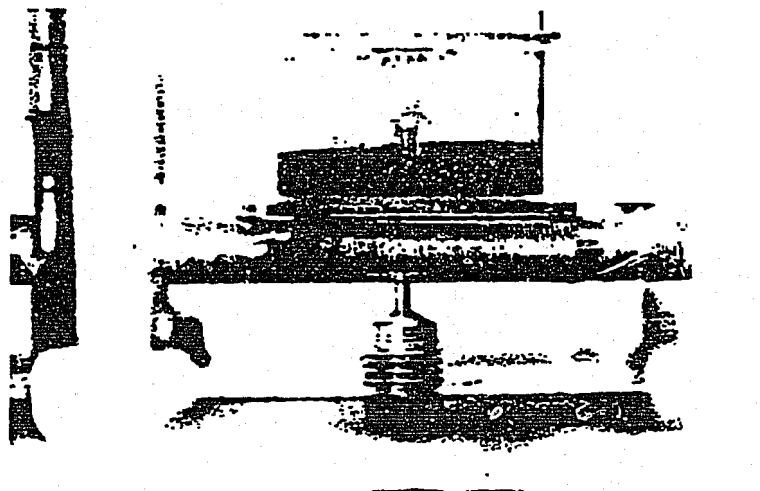
Figure 5.44. A Photograph of the Static Bed-Height of the
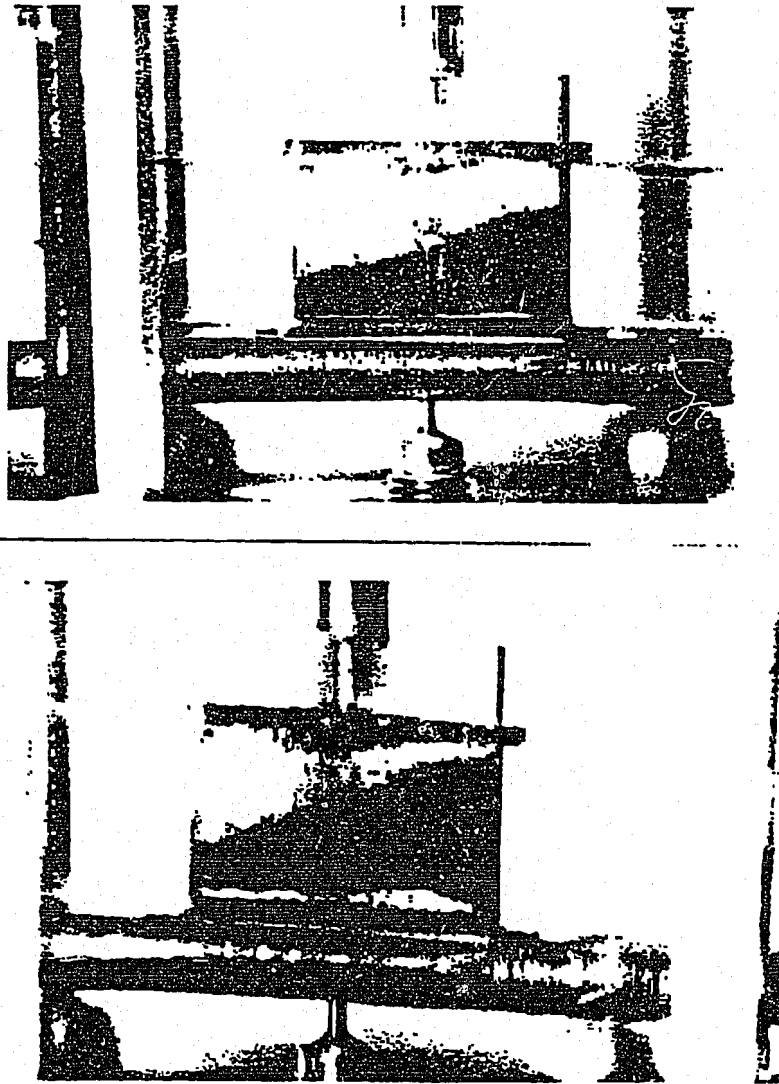Cold-Flow Microreactor Model.

Figure 5.45. A Vibrofluidized-Bed of Fused-Iron Catalyst
at a Gas Velocity Well Below the Minimum Gas-
Fluidization Velocity.

when the velocity of the feed gas passing through the catalyst zone is well below the minimum gas-fluidization velocity. This is the case for the three flow rates (417, 833, and 1650 actual mm^3/sec) used for gas mixing studies in the cold-flow model experiments as well as the flow rate used in the steady-state F-T synthesis experiments (411 actual mm^3/sec).

Table 5.2 summarizes calculated minimum fluidization velocities for gases of interest at conditions of interest. The values obtained for helium and argon correspond to observed values of minimum fluidization velocity in the cold-flow model.

The photographs in Figure 5.45 show that the catalyst bed actually lifts off from the distributor plate as the microreactor vibrates. In addition, catalyst particles can be seen airborne at the top surface of the catalyst mass. There is an intense circulation of catalyst particles in the reaction zone at this point. Also note that the bed slants toward one end of the reaction zone. At low gas velocities, this tends to happen, unless the microreactor was perfectly level and the tension on all three flexible metal hoses as well as on the leaf-springs are equal.

As the linear gas velocity through the catalyst bed is increased, the bed height begins to level out and then oscillate. Oscillation usually occurs at gas velocities greater than one-half of the minimum gas-fluidization velocity. Figure 5.46 shows the vibrofluidized bed as it oscillates. In this picture, the left-hand side of the bed is falling as the right-hand side is rising. In turn, the left-hand side will strike the distributor plate and start to rise as the right-hand

TABLE 5.2

Calculated Minimum Gas-Fluidization Velocities for Gases Used in the
Cold-Flow Microreactor Model and Fischer-Tropsch Synthesis
Microreactors (Refer to Appendix A for Method of Calculation).

Gas	Conditions		Minimum Gas-Fluidization Velocity, v_ϵ (m/s)	Flow Rate Corresponding to v_ϵ (actual mm^3/s)
	Temperature (°C)	Pressure (kPa)		
Helium	20	101	0.22	17,700
Argon	20	101	0.24	19,200
Hydrogen	400	2,230	0.29	23,300
Carbon Monoxide	400	2,230	0.08	6,390
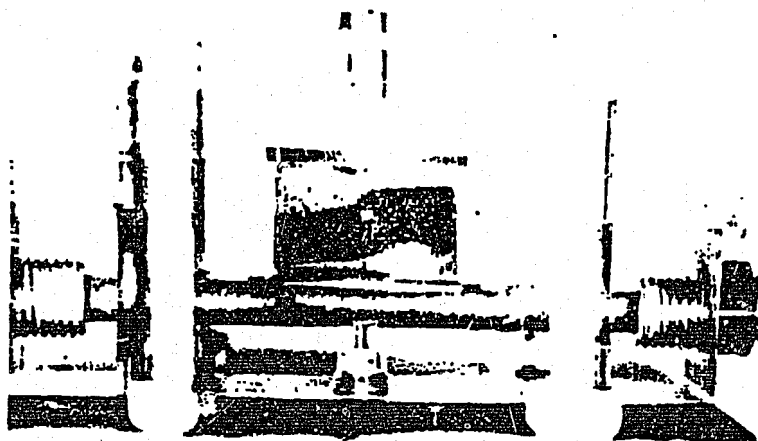
Figure 5.46.   The Oscillation of a Vibrofluidized-Bed
of Fused-Iron Catalyst.

side peaks out and begins to fall. One full bed-oscillation cycle involves two cycles of the distributor plate. This suggests that the bed oscillates at approximately 12 cycles per second. In real time, the alternate rising and falling of the two sides of the catalyst bed produce the illusion of a half-cycle cosine wave. Indeed, at slightly higher velocities, a full-cycle sine wave has been observed.

As the gas velocity through the catalyst bed surpasses the minimum gas-fluidization velocity, the bed technically is classified as a vibrated fluid-bed rather than a vibrofluidized bed. Figure 5.47 shows a series of pictures taken of the vibrated fluid-bed. The catalyst bed has become more dilute and bubbles can sometimes be identified. The bed continues to strike the distributor plate and then lifts off from it. As can be seen in these photographs, the bed has expanded to the point of nearly filling the entire reaction zone. Velocities above the minimum gas-fluidization velocity are much too high to be considered for use in the F-T synthesis studies presented here. Vibrofluidized beds, such as those shown in Figures 5.45 and 5.46, allow for the use of low feed-gas velocities, while the intense particle mixing of a gas fluidized-bed is still obtainable.
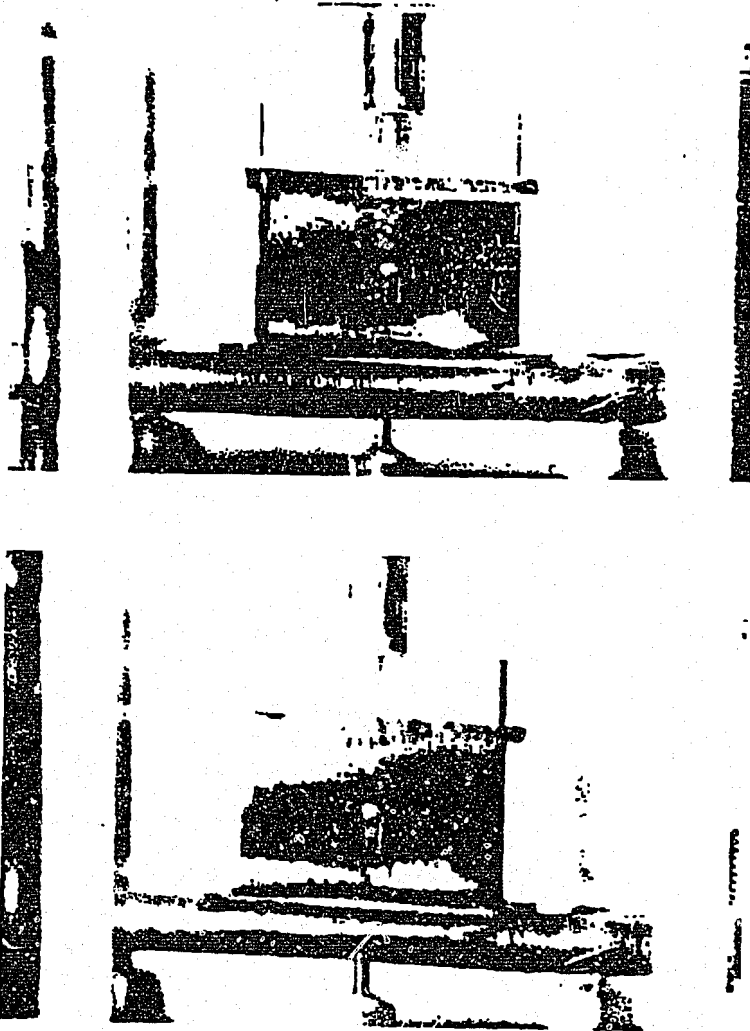
Figure 5.47. A Vibrated Fluid-Bed of Fused-Iron Catalyst.
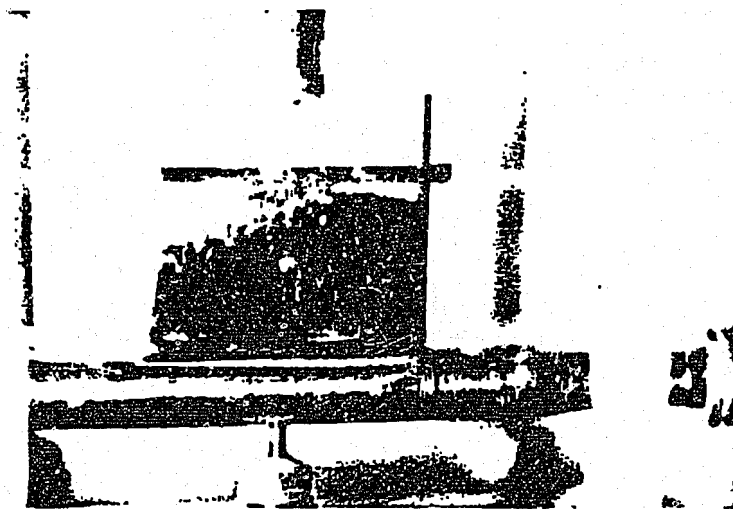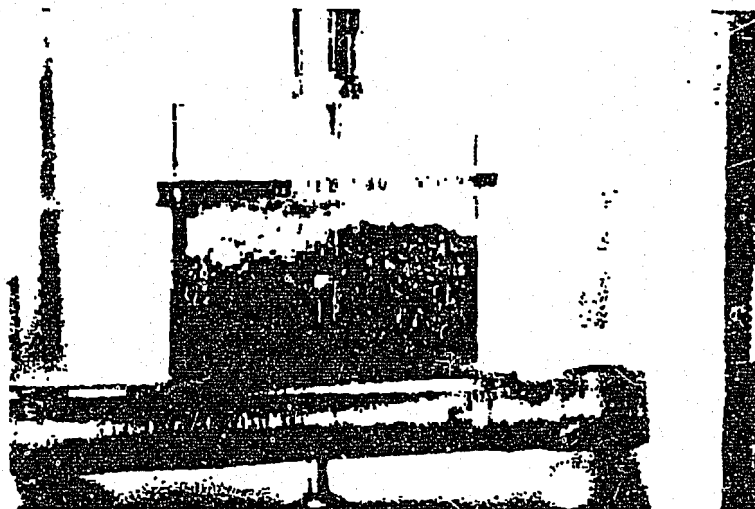The Gas Velocity Is Above the Minimum Gas-
Fluidization Velocity.

Figure 5.47. (Continued)

CHAPTER 6

DESIGN AND CONSTRUCTION OF A VIBROFLUIDIZED-BED MICROREACTOR SYSTEM FOR UNSTEADY-STATE FISCHER-TROPSCH SYNTHESIS

6.1 Experimental Apparatus and Procedure

6.1.1 Experimental Apparatus

A vibrofluidized-bed microreactor system was designed and constructed for the study of unsteady-state Fischer-Tropsch synthesis. The goal was to provide for rapid feed-gas switching on the order of seconds at temperatures approaching 400°C and pressures of 2,220 kPa (323 psia). In order to do this, a microreactor system similar in concept to the cold-flow sliding-plug vibrofluidized-bed model was constructed.

The purpose of the study was to rapidly switch between a feed gas of a high H_2/CO ratio (F-gas) and another feed gas of a low H_2/CO ratio (S-gas) so as to simulate the residence time of the iron catalyst in the supernatant and fluidizing zones of a "heat-tray" reactor (see Figure 1.1). The effect of catalyst exposure to the rapidly changing partial pressures of hydrogen and carbon monoxide will be studied with emphasis on reduction of the rate of carbon deposition.

Figure 6.1 shows two photographs of the system. Figure 6.2 is a schematic diagram of microreactor system.

Hydrogen and a premixed synthesis gas containing hydrogen, carbon monoxide and argon enter the system through high-pressure regulators (Airco model 49). The feed gases, "F-gas" and "S-gas", then pass through an activated-carbon filter used to remove impurities. The carbon filters
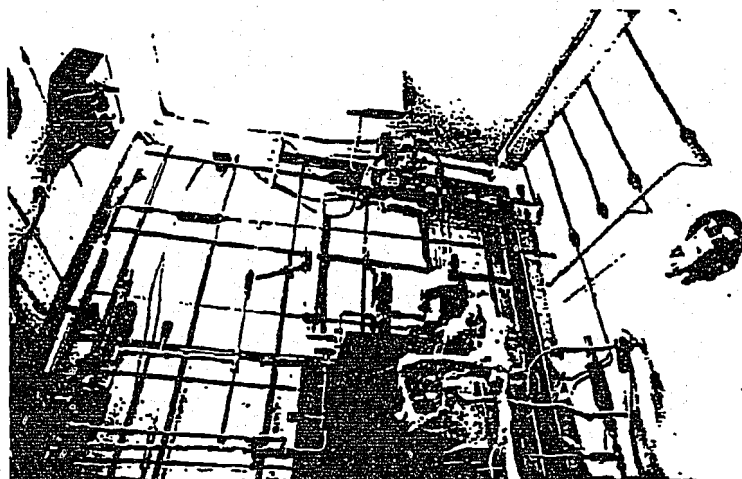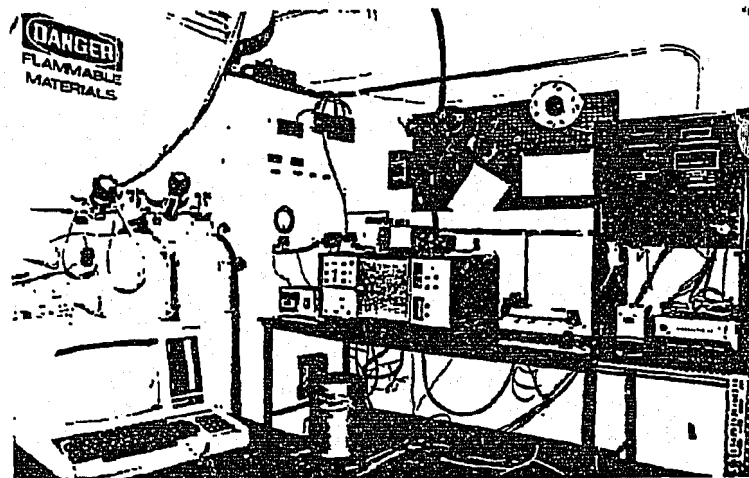
Figure 6.1. Photographs of a Sliding-Plug Vibrofluidized-
Bed Microreactor System for Unsteady-State
Fischer-Tropsch Synthesis.

Top: Control and Analysis Systems.
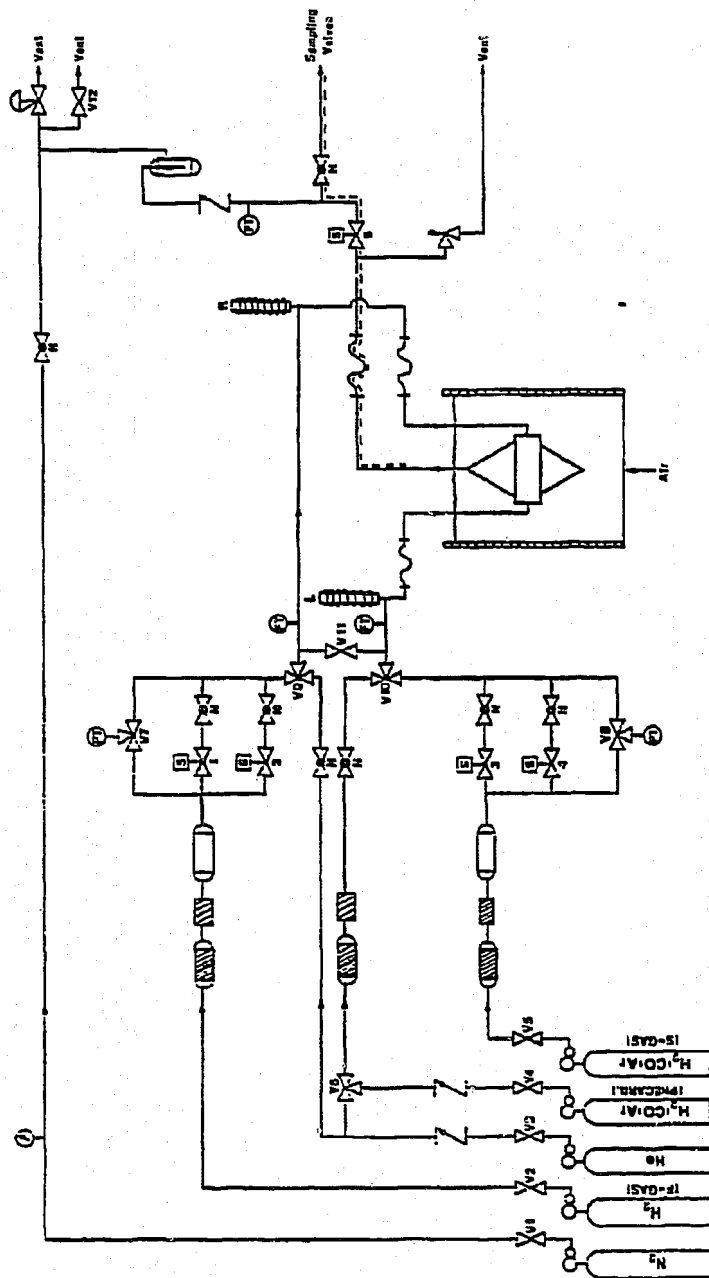Bottom: Microreactor System.

Figure 6.2.   A Sliding-Plug Vibrofluidized-Bed Microreactor System for Unsteady-State Fischer-Tropsch Synthesis.   (See Figure 4.1b for Equipment Symbols).

are followed by a 15-micron sintered stainless-steel element filter which protects the downstream equipment, such as needle and solenoid valves. Two 1000-ml sample cylinders (304- stainless-steel) act as reservoirs, storing the gas upstream of solenoid valves 1-4.

Two-way, normally-closed, high-pressure, stainless-steel solenoid valves manufactured by Circle Seal Controls (model SV10) control the flow of feed gases to the microreactor. The needle valves associated with these solenoid valves are low-flow stainless-steel types made by Nupro. Series SG needle valves are used in conjunction with solenoid valves 1 and 3, and are typically only used for gas purging before an experiment. Series SGD double-needle valves associated with solenoid valves 2 and 4 are used to set feed-gas flow rates in conjunction with a thermal mass flow meter (Brooks model 5810). The range of this flow meter is 0-2000 standard cm^3/min. A critical pressure drop is again maintained across the needle valves so that feed-gas flow rates are independent of downstream pressures.

Three-way valve V9 allows helium to be directed to the sliding-plug microreactor for gas purging before and after an experiment. Similarly, three-way valve V10, in association with three-way valve V6, can be used to direct helium for purging, or a feed gas of high H_2/CO ratio for precarburization of the catalyst to the microreactor. A manual shut-off valve V11, connects the two feed streams that lead to the microreactor. This valve is opened only before and after, but never during an experiment. Its purpose is to produce a balanced pressure across the sliding-plug during the purging procedure.

Three-way valves V7 and V8 allow selection of either the pressure upstream or downstream of the needle valves. Pressures are monitored at these points using absolute-pressure transducers of the strain-gage type (Schaevitz Model P721) with a range of 0-6,893 kPa. The sliding-plug microreactor is suspended into a constant-temperature bath (Techne SBL-2D) as described in Section 4.1.1.

Flexible stainless-steel hoses connect the vibrating sliding-plug microreactor to the stationary feed-gas lines and solenoids. A 0.356-mm stainless-steel wire connects the plunger inside each solenoid, labeled by L and R in Figure 6.2, to the sliding plug in the plenum zone of the microreactor. Feed gases enter this section of the system at a "tee"-union directly below the solenoids.

The product-gas exit section of the microreactor is identical to that for the steady-state system described in Section 4.1.1. Product gases exit the reactor via a stainless-steel line heated to 200°C. Solenoid valve 5 is a high-temperature, high-pressure, normally-closed stainless-steel valve manufactured by Atkomatic Solenoid Valves. This solenoid valve is held open continuously during catalyst reduction and synthesis.

An over-pressure relief valve (Nupro model 4CA) set for 4,135 kPa has been placed upstream of solenoid valve 5 as a safety precaution. A small amount of product gas is drawn off continuously via a double-needle valve (Nupro SGD) and a 1/16-inch O.D. stainless-steel tube. This line is heated to 200°C and reduces the gas to nearly atmospheric pressure before it flows through the sampling valves associated with the gas chromatograph. After

passing the sampling point, the product gas goes through a check valve and into a liquid trap.

The system pressure is maintained at 2,220 kPa through the use of a back-pressure regulator manufactured by Circle Seal Controls (model BPR-8A). Nitrogen is used as a ballast gas in order to maintain a constant system pressure as described in Section 4.1.1. Valve V12 is a manual shut-off valve used to bleed down the system pressure at the end of an experiment.

All equipment and tubing in contact with hydrogen or synthesis gas are constructed of either 304- or 316- stainless steel. The solenoid plungers and stops are made of 416- stainless steel which is magnetizable. Regulators and tubing coming in contact with only helium or nitrogen are made of brass.

In general, all tubing is 316- stainless steel, 1/4-inch O.D. with a 0.035-inch wall thickness. The maximum safe working pressure of this system at 21°C is approximately 7,000 kPa.

6.1.1.2 A Sliding-Plug Vibrofluidized-Bed Microreactor

The design and construction of the sliding-plug vibrofluidized-bed microreactor for F-T synthesis is based in part on the design of the steady-state microreactor (Section 4.1.1.2) and in part on the design of the cold-flow model (Section 5.1.1.2). Figure 6.3 shows photographs of the microreactor. Figures 6.4 and 6.5 are schematic cross-sectional front and side views of the sliding-plug microreactor.
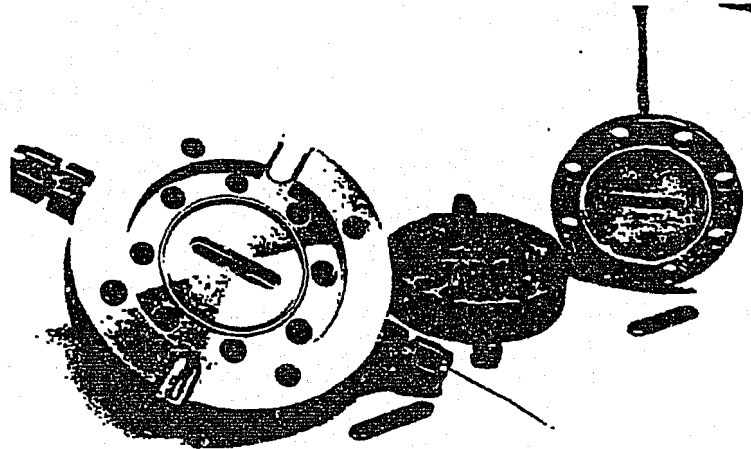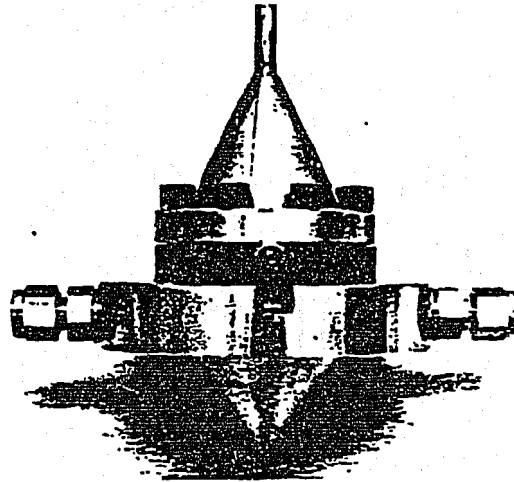
Figure 6.3. Photographs of the Sliding-Plug Vibrofluidized-
Bed Microreactor for Unsteady-State F-T
Synthesis: (a) The Assembled Microreactor
Less Feed-Line Tubing; (b) The Microreactor
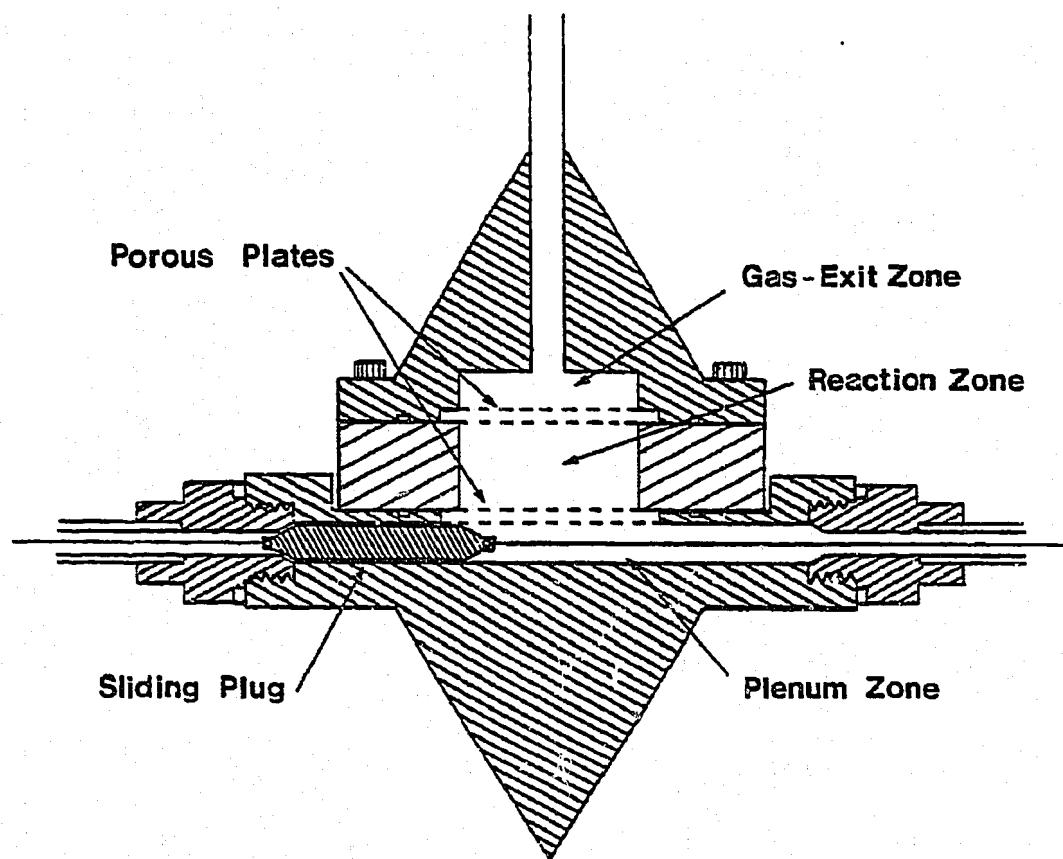Base Section, Reaction Section and Gas-Exit
Section.

Porous Plates

Gas-Exit Zone

Reaction Zone

Sliding Plug

Plenum Zone

Figure 6.4. A Schematic Cross-Sectional Diagram
of the Sliding-Plug Microreactor.
(Front View).

Gas-Exit Zone

Reaction Zone

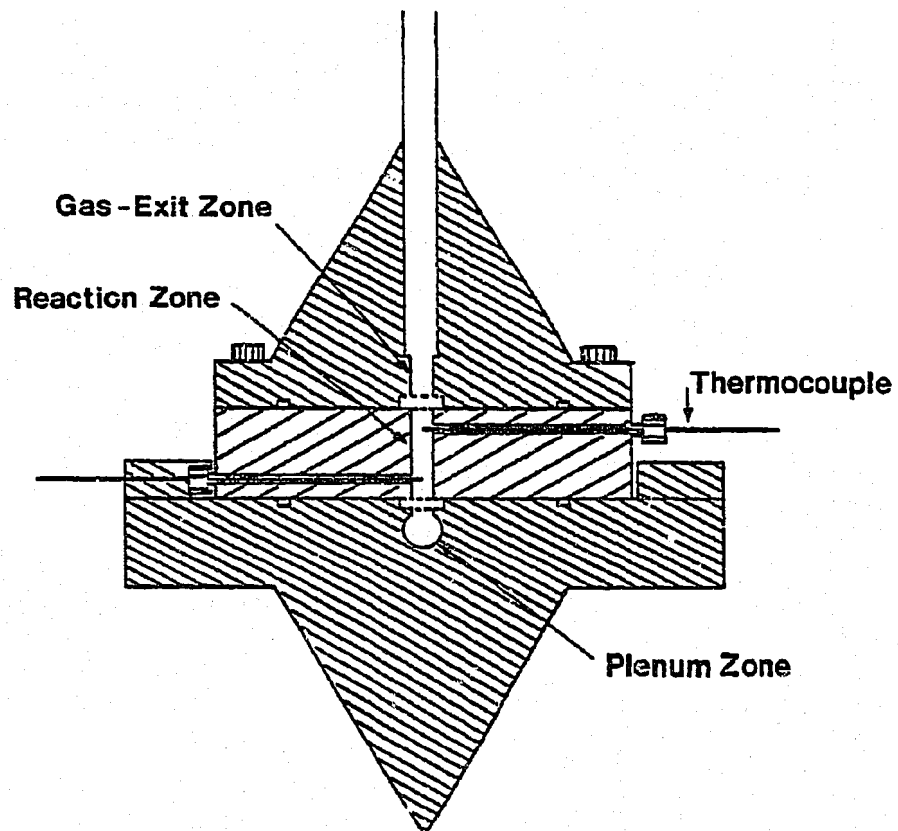**Thermocouple**

Plenum Zone

Figure 6.5. A Schematic Cross-Sectional Diagram of the Sliding-Plug Microreactor. (Side View).

As before, the microreactor consists of three sections: (1) the base (plenum) section, (2) the reaction section; and (3) the product-gas exit section.

The base section consists of a 6.35-mm hole drilled horizontally through the conically shaped piece of 316- stainless steel. The center line of the hole lies 4.76 mm below the top surface of the base section. A 3.175-mm wide slot, 24.5-mm long, has been milled down into the drill hole from the top. A wider slot, 6.35-mm wide and 31.75 mm in length, has been milled 1.59-mm deep along the same line as the 3.175-mm wide slot. This creates a lip 3.175-mm wide around the smaller slot. This lip supports a 2-micron sintered stainless-steel distributor plate. Both slots have rounded ends as shown in Figure 6.3.

The horizontal drill-hole in the base section is, as before, the plenum zone. The plenum zone is 76.20 mm in total length. The material surrounding each end of the plenum has been tapped with straight threads. A straight-thread male connecter (Swagelok 7/16-20) is screwed into each end. These connectors serve as plug stops for the sliding plug in the plenum zone. The inner surfaces of the connectors have been tapered to approximately a 30-degree angle to mate with the sloping plug.

A gas-tight seal is maintained between the connector and the base section through the use of a copper washer. The washer thickness has been selected so that when the connector is tight, the inner end will just be touching the end of the plenum.

The sliding-plug itself is made of 316- stainless steel 6.22 mm in diameter and 34.93 mm in total length. A small hole has been drilled in each end of the plug to allow for connections to the solenoid plungers via a 0.356-mm stainless-steel wire.

The reaction section of the microreactor is made from a piece of 316- stainless steel, 63.50 mm in diameter and 14.29-mm thick. A 3.175-mm wide slot, 25.4-mm long, has been milled in the reaction section, creating the "reaction zone." As seen in Figure 6.5, two thermocouples monitor the temperature in the reaction zone. Two holes, 1.59 mm in diameter, have been drilled perpendicular to the length of the reaction-zone slot. 1/16-inch Swagelok stainless-steel male connectors have been modified and welded to reaction section.

A type "J" thermocouple with a 1/16-inch O.D. stainless-steel sheath has been inserted through each connector into each hole. In this way, a gas-tight seal is maintained. The thermocouples are 635.0 mm in total length and are attached to connectors outside of the constant-temperature bath. One thermocouple enters the reaction zone 3 mm above the distributor plate and the other 3 mm below the catalyst retention plate. Therefore they are approximately 8.29 mm apart.

The gas-exit section of the microreactor is conical in shape. A slot, 3.175-mm wide and 25.4-mm long, has been milled to a depth of 7.94 mm in this section. As is similar to the base section, a recessed area has been machined to accept a sintered stainless-steel catalyst retention plate (1.59-mm thick and 20-micron type). The recessed area is 6.35-mm wide and 31.75-mm long, with rounded ends creating a

small lip for the plate to rest on. A 1/4-inch O.D. stainless-steel tube with a 0.035-inch wall thickness has been inserted down from the top, and it breaks through the slot in the gas-exit section. This tube has been welded at the peak of the cone to insure a leak-proof seal.

The reactor maintains a gas-tight seal even against hydrogen through the use of two silver-plated stainless-steel O-rings. The O-rings are part number MS9373-047 as supplied by American Seal and Engineering Co. An O-ring groove has been machined into the base and gas-exit sections of the microreactor. Each groove is 44.69 mm ±0.06 mm O.D., 39.70 mm I.D. and 1.13 ±0.06 mm deep. Eight 1/4-28 cap screws provide enough clamping force to smash the O-ring in their grooves. The base section has been tapped to accept these screws. The gas-tight seal is created by the gas pressure, forcing the O-ring against the outer surface of the groove and against the mating surface. The silver plating tends to fill any defects and prevents hydrogen from leaking.

The vibrating system is identical to the one described in Section 4.1.1, with the exception of the way in which the threaded rods are attached to the microreactor. In the sliding-plug microreactor, 1/4-inch threaded rods are screwed directly down into tapped holes in the base section. Figure 6.3 shows these four holes.

6.1.1.3 Solenoids

The solenoids controlling the movement of the sliding plug are an integral part of the microreactor system. Figure 6.6 shows a schematic cross-sectional view of a solenoid.